EVALUATION OF GLOBAL PRECIPITATION MEASUREMENT (GPM) SATELLITE PRODUCTS OVER SAUDI ARABIA

BY

MOHAMMED MAHMOUD

A Thesis Presented to the
DEANSHIP OF GRADUATE STUDIES

KING FAHD UNIVERSITY OF PETROLEUM & MINERALS

DHAHRAN, SAUDI ARABIA

In Partial Fulfillment of the
Requirements for the Degree of

MASTER OF SCIENCE

In

CIVIL ENGINEERING

May 2017

KING FAHD UNIVERSITY OF PETROLEUM & MINERALS

DHAHRAN- 31261, SAUDI ARABIA

DEANSHIP OF GRADUATE STUDIES

This thesis, written by MOHAMMED TARIG MOHAMMED MAHMOUD under the direction of his thesis advisor and approved by his thesis committee, has been presented and accepted by the Dean of Graduate Studies, in partial fulfillment of the requirements for the degree of MASTER OF SCIENCE IN CIVIL ENGINEERING.

Dr. Muhammad A. Al-Zahrani
(Advisor)

Dr. Salah Al-Dulaijan
Department Chairman

Dr. Hatim Sharif
(Member)

Dr. Salam A. Zummo
Dean of Graduate Studies

Dr. Shakhawat Chowdhury
(Member)

23/5/14

Date

Dedication

I dedicate this thesis to my lovely parents Mrs. and Mr. Mahmoud, I hope this humble effort will complete the dream that you had for me, to my lovely wife, for her patience, her advice, her support, and her faith.

ACKNOWLEDGMENTS

All praises and worship are for ALLAH, I seek His help and ask for His forgiveness, I thank Him for providing me with knowledge and I always strive to achieve His reward.

First and foremost, I would like to pay a high tribute to my thesis advisor Dr. Muhammad A. Al-Zahrani for accepting me under his supervision. During my research, he contributed to a rewarding graduate school experience by giving me intellectual freedom in my research, engaging me in innovative ideas, and always demanding a high quality of work in all my endeavors. His supervision was paramount in providing a well-rounded experience which I can rely on in my long-term profession goals. I always admired his knowledge, intuition, and vision. For everything you've done for me, Dr. Al-Zahrani I thank you.

I would like to gratefully and sincerely thank Dr. Hatim Sharif for his invaluable guidance, continuous support, unremitting follow-up, and for providing me a profound knowledge through interesting ideas and most importantly, his friendship during my research. I would like to thank him also for proposing the idea of our thesis and his valuable effort towards the completion of this research. Additionally, I would like to thank my committee member Dr. Shakhawat Chowdhury for his support and his interest in my work.

I owe a deep appreciation to Dr. Ashraf Farahat for introducing me to various research opportunities during my master, not to mention his valuable time that he shared with me. I am thankful for his valuable suggestions and his constant help and encouragement.

I gratefully acknowledge King Fahd University of Petroleum and Minerals for providing me an opportunity to pursue my master degree in the high standard environment. Also, I am deeply thankful for all Civil and Environmental engineering faculty and staff for supporting me during my studies.

Finally, and most importantly, I am grateful to my wife Safa. Her faith, advice, encouragement, patience, and untiring love were irrefutably the power I need me fulfill my dreams. Also, I would like to acknowledge my lovely parents, my sister and brother for their indefatigable love and absolute support in all my life aspects. You made my life unique, carefree and successful and made me who I am now. Also, I am gratitude to my friends who shared with me all difficult moments and provide me with unconditional support.

TABLE OF CONTENTS

LIST OF TABLES

LIST OF FIGURES

ABSTRACT

Full Name : Mohammed Tarig Mohammed Mahmoud

Thesis Title : Evaluation of Global Precipitation Measurements (GPM) satellite products over Saudi Arabia

Major Field : Civil and Environmental Engineering

Date of Degree : May 2017

Hydrologic analysis and modeling require reliable and accurate precipitation data for successful simulation. The measurements of precipitation should be more representative of the true precipitation. Many approaches and techniques have been used to collect precipitation data. Recently, hydrometeorological and climatological applications of satellite precipitation products are witnessing a significant leap with the emergence of the latest satellite product; namely, Integrated Multi-satellitE Retrievals for Global Precipitation Measurement (IMERG) product which can be utilized to predict and analyze precipitation data.

This research focus on the validation of the IMERG satellite rainfall products: early, late and final runs, using ground-based rain gauge observations for all regions of Saudi Arabia over the period from October 2015 to April 2016. The accuracy of each IMERG product was assessed using six statistical matrices to perform three main evaluations: regional evaluation, event-based evaluation and station-based evaluation. The results indicate that the early run product performed well in the middle, eastern and some parts of the western region while the other parts the accuracy of the satellite estimation is flocculating between overestimating and underestimating the precipitation. The late run product showed an

improvement in the accuracy of the satellite estimation for the southern and western parts; however, the northern and the middle parts of Saudi Arabia still suffer a relatively high error of estimation. The final run product, revealed a significant improvement of precipitation estimation and success to obtain a high accuracy in estimating precipitation for most parts of the Kingdom.

Furthermore, this study provides a comprehensive evaluation of the GPM IMERG early, late and final run products, which could provide a valuable reference for the performance of the GPM satellite in arid and semiarid areas. Also, it could be used as a beneficial reference in future development of the IMERG algorithms.

ملخص الرسالة

الاسم الكامل: محمد طارق محمد محمود

عنوان الرسالة: تقييم قياسات الامطار بواسطة الأقمار الصناعية العالمية (GPM) في المملكة العربية السعودية

التخصص: هندسة مدنية

تاريخ الدرجة العلمية: مايو 2017

يتطلب التحليل والنمذجة الهيدرولوجية بيانات أمطار موثوقة ودقيقة للمحاكاة الناجحة. وينبغي أن تكون قياسات الامطار أكثر تمثيلا لكمية المطر الحقيقي الذي سقط على المنطقة المعينة. وعادة تستخدم العديد من الطرق والتقنيات لجمع بيانات هطول الأمطار. وفي الآونة الأخيرة، تشهد تطبيقات الأرصاد الجوية الهيدرولوجية والمناخية لقياسات الامطار باستخدام الساتلايت مع ظهور أحدث منتج لقياس الامطار بالساتلايت؛ وهو - الاسترجاع المتكامل المتعدد الساتلايت من أجل قياسات الامطار العالمية (IMERG) - الذي يمكن استخدامه للتنبؤ وتحليل بيانات هطول الأمطار.

ويركز هذا البحث على التحقق من صحة منتجات هطول أمطار باستخدام الساتلايت (IMERG) وهي منتج القياس المبكر، منتج القياس المتأخر ومنتج القياس النهائي بمقارنتها بقياسات الامطار الأرضية لجميع مناطق المملكة العربية السعودية خلال الفترة من أكتوبر 2015 إلى أبريل 2016. هذا وان دقة كل منتج من منتجات (IMERG) تم تقييمها باستخدام ستة قياسات إحصائية لأداء ثلاثة تقييمات رئيسية، التقييم الإقليمي، والتقييم القائم على الحدث والتقييم القائم على المحطة.

وتشير النتائج إلى أن أداء منتج القياس المبكر كان جيدا في وسط وشرق وبعض الأجزاء الغربية من المملكة في حين أن أجزاء أخرى أظهرت النتائج ان دقة تقدير الأقمار الصناعية متذبذبة بين المبالغة والتقليل في تقدير هطول الأمطار. وأظهر منتج القياس المتأخر تحسنا في دقة تقدير الساتلايت للجزء الجنوبي والغربي، إلا أن الجزء الشمالي والمنطقة الوسطى من المملكة العربية السعودية لا يزالا يعانيان من خطأ مرتفع نسبيا في التقدير. أما المنتج النهائي، فقد كشف عن تحسن كبير في تقديرات هطول الأمطار ونجح في الحصول على دقة عالية في معظم أنحاء المملكة العربية السعودية.

وعلاوة على ذلك، توفر هذه الدراسة تقييما شاملا للساتلايت (GPM) – ومنتجاته (IMERG) وهي منتج القياس المبكر، منتج القياس المتأخر ومنتج القياس النهائي، والتي يمكن أن توفر مرجعا قيما لأداء الساتلايت (GPM) على المناطق القاحلة وشبه القاحلة. كما يمكن استخدامه كمرجع مفيد في التطوير المستقبلي لخوارزميات (IMERG).

CHAPTER 1

INTRODUCTION

1.1 Background

In general, the term precipitation refers to all formations of moisture falling onto the ground and originating from clouds. In the hydrologic cycle (figure 1), it is that part in which atmospheric water vapor is condensed, resulting in water droplets which are large enough to fall to earth by gravity. There are many forms of precipitation, which differ according to their metrological conditions. Moreover, precipitation is one of the most vital components of the global energy and water cycles [1, 2].

Measurement of precipitation provides primary input information for hydrological, meteorological and climatic models, which are used to estimate the reaction of the hydrological system due to natural hazards resulted from excess precipitation for instance landslides, flood, and droughts [3, 4]. The response of the hydrological system depends on many factors such as precipitation spatial pattern, land coverage, intensity and duration [5, 6]. Precipitation is considered to be a key forcing factor in many climatic and hydrometeorological applications, therefore, measuring of precipitation precisely with high spatiotemporal resolution is always challenging due to its spatial and temporal variation and its complex distribution. In addition, observing and measurement of precipitation are critical to our well-being; excess rainfall threatens life and property, whereas a smaller amount of rainfall causes droughts that affect our agricultural systems and can cause starvation. Another interesting fact is that precipitation has a financial value since it is a

significant factor in water resources management and agribusiness [1, 7, 8]. The development of the landscape was rolled by precipitation, both through erosional processes and by supporting the natural vegetation; it is also an element that contributing on the transport of nutrients and pollution, and also in the disposition of atmospheric pollution [9].

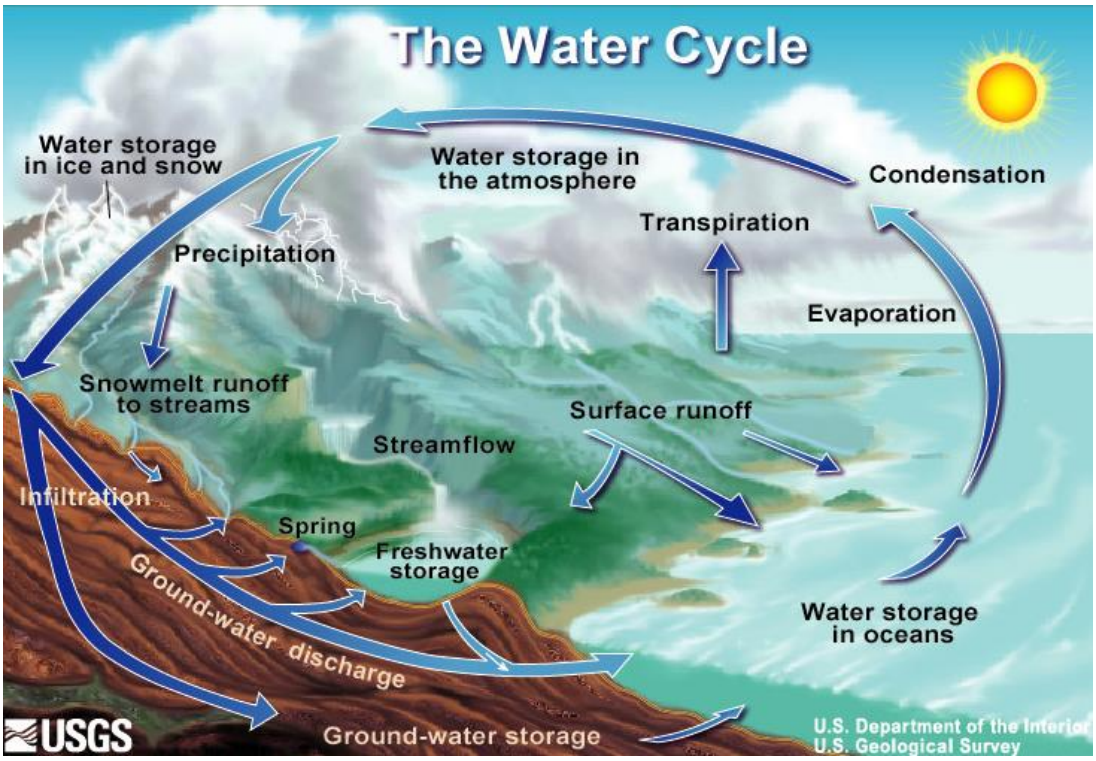

Figure 1: The hydrologic cycle (USGS).

1.2 Precipitation in Saudi Arabia

The Kingdom of Saudi Arabia is located between latitudes 16°21’58’’N and 32°9’57’’N, and longitudes 34°33’48’’E and 55°41’29’’E as shown in figure 2. This location falls in the tropical and subtropical desert regions of the globe [10, 11]. The Kingdom has a dry desert climate, with generally light winds and high temperatures in most regions.

In Saudi Arabia, each season has different weather features which the rain allied on. Generally, summer rain resulted by the Intertropical Convergence Zone and the northward advance of the southwesterly monsoon [12]; their effect declines from north to south, not including highlands where the uplift factor is dominant [10, 13]. On the other hand, the winter rain is produced by westerly waves in the upper atmosphere and disturbances from the Mediterranean Sea and the Sudan Trough [10]. The spatial and temporal variations of the precipitation amount are a major consideration for widespread designs of water projects and other activities.

Regional and local climate are exaggerated by large-scale atmospheric movement along with the features of the surface. Besides, atmospheric movement changes and variations are important aspects of the climate [14]. The features of the rainfall vary locally and regionally based on the patterns of the atmospheric circulation resulted by the El Niño Southern Oscillation (ENSO), North Atlantic Oscillation (NAO), and other variability patterns [10, 14, 15].

In general, the rainy season in Saudi Arabia occurs between October and April [14 – 16], during which the rain is described as scarce and irregular rain. For the other months, light precipitation observed in several parts of Saudi Arabia except for the southwestern region

which suffers from a high spatial variation, due to the topography of the area (mountain area) [15]. The topographically driven convective rain in the southwestern region resulted in multi-rain events in this specific region of Saudi Arabia [11, 17, 18]. Overall, in desert areas, the mean annual precipitation is less than 100mm while in mountain areas it is ranging between 250-300mm [10, 11, 14].

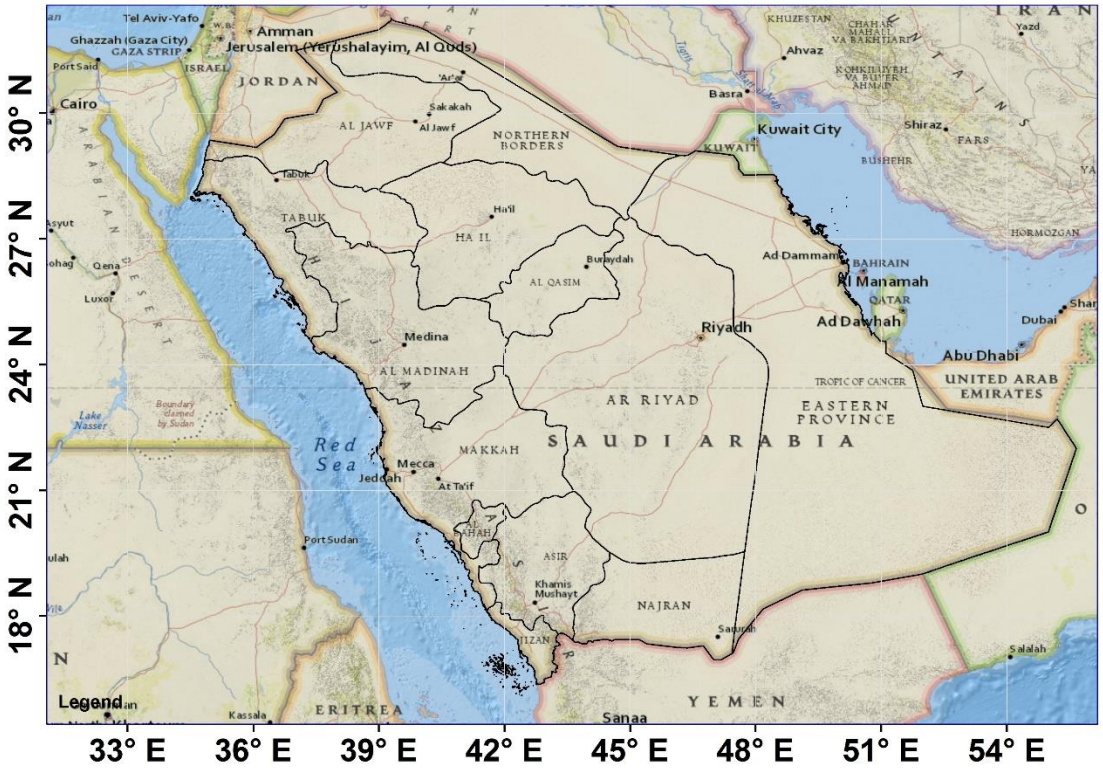

Figure 2: Map of Saudi Arabia and its administrative regions.

1.3 Objectives of the Research

In recent years, many researchers indicated that earth observing satellites perform well in measuring or estimating the precipitation rates and are also able to represent the spatiotemporal variations of precipitation for most parts of the World with high resolution [19 – 21]. However, these satellites need to be assessed using the ground observations in order to verify the accuracy of their precipitation measurement products [21 – 23].

This study intended to explore and evaluate the accuracy of GPM day-1 IMERG "Early, Late and Final" run precipitation products using daily ground-based observations data as a reference in the whole regions of the Kingdom of Saudi Arabia over the period of October from 1st, 2015 to April 30th, 2016. The main objectives of this research include the following:

1. Evaluate the accuracy of the IMERG products under the effect of regional and national scale comparison.
2. Evaluate the heterogeneity of the rainfall distribution over Saudi Arabia using station-based comparison.
3. Evaluate each major storm event that occurred during the study period separately to reveal the differences between IMERG products.

1.4 Thesis Organization

This thesis is divided into six chapters. The first chapter gives an introduction of the research, general background about the precipitation in Saudi Arabia and the objectives of this study. Chapter two provides an up-to date review of previous studies and research related to precipitation measurement approaches, rain gauge observations and types, satellite measurement techniques and the GPM satellite and its products. The features of the study area, the statistical metrics used to evaluate the satellite data and the precipitation datasets used in this study, are presented in chapter three. Chapter four presents the detailed methodology that has been adopted to perform the evaluation process, starting from the data acquisition, processing, analysis and the comparison process. Chapter five presents the assessment results which test the accuracy of the GPM satellite data of three main scale evaluations, namely: regional-based, station-based and event-based. The last chapter summarizes the outcome of this study, draws conclusions and implications, and suggests recommendations for future research opportunities.

CHAPTER 2

LITERATURE REVIEW

2.1 Precipitation Measurements

In literature, there are many techniques and instruments that have been developed for collecting and estimating precipitation. Measuring and monitoring accurate precipitation amount and intensity are the most important steps before performing any analysis or constructing hydrologic models [24]. The precipitation measurements are essential for flood forecasting, flood alert, availability of water resources assessment, design of hydraulic structures, and other numerous hydro-applications.

Presently, there are three main methods which can be used to measure precipitation namely: ground measurements (i.e. rain gauges), weather Radar measurements and satellite estimates [3]. Rain gauges try to quantify by direct measurement, the flux of the drop size distribution. While weather radar and satellites attempt to detect the special distribution of the drop size above the surface.

2.2 Ground observations

The precipitation observed on the ground using three popular platforms, rain gauges, disdrometers, and ground radar. Globally, rain gauges can provide a direct measure of precipitation and are considered as the ground truth for precipitation observations for a given observation point. Disdrometers is considered one of the recently developed instruments that measure the total precipitation amount as well as estimating the relative

drop size distribution (DSD) which is playing a major role in estimating the precipitation using a microwave-based method [9, 25]. Although rain gauges and disdrometers provide a direct measurement, they considered having relatively small sampling area, which decreases the accuracy when dealing with the measured value as a representative measurement. On the contrary, ground or weather radars estimate the precipitation using an indirect observation based on the backscattered echo, which has a large sampling volume.

2.2.1 Rain gauges

Although rain gauges measure a point precipitation, it can be utilized also by distribution a group of them to measure the rainfall flux. However, a group of rain gauges located in a small portion of the ground most probably to measure a similar rainfall flux based on the distance between each measuring sites [9]. Rainfall rates drop size distribution, and rainfall accumulation measured by gauges located on a few meters difference are expected to be the same. It is expected that when the distance increases the correlation between these gauge measurements decreases.

There are many types of recording gauge. However, only three of them are commonly used for measuring precipitation which are the tipping bucket gauge, the universal weighing-type gauge, and float-type gauge. Nonetheless, gauge data have many potential errors which can be summarized as follows: (1) underestimation of heavy precipitation, (2) instrumental problems and (3) external factors such as the wind, evaporation by rising in the temperature [25]. In addition, precipitation measurement represents a point value and not an areal measurement, so it will not be able to describe the spatiotemporal variation of precipitation. In the following paragraphs, the recording gauges are presented briefly.

2.2.1.1 Tipping bucket gauge

The most common rain gauges are tipping buckets. Typically, it consists of the accumulating area which holds the collected rain and it drains into fluctuating buckets. When a bucket is filled, a cantilever mechanism resulted in a bucket to discharge the collected rain and produce an electric signal (figure 3). This process is repeated when another bucket starts to fill. The rainfall rate can be calculated by multiplying the opening area of the gauge collector by the resultant division of the constant volume of the bucket over the time between tips [9, 26, 27].

Although the tipping bucket is a fairly simple mechanical instrument, it is subjected to a potential source of errors which affects its accuracy. Most of the tipping bucket gauges underestimate the heavy precipitations, due to the small opening or collection area, which cause the bucket to fill faster resulting in mechanical errors. These mechanical errors can lead to a saturation effect, which is the case when the gauge cannot be able to drain the collected rain. In addition, high rainfall rates can affect the time required by the bucket to fill and dump the collected water. This fast repeated process of filling and dumping resulted in a loss of water during the accumulation process [9, 25–27, 29]. Another frequent source of error that affects the tipping bucket gauges is blocking and clogging of mechanism due to birds, bugs or anything has the ability to harm or localize into the mechanism, this can happen when these gauges are not used for a long time.

The effect of the above mentioned and discussed errors can be reduced by providing a continuous assessment and maintenance as well as performing an accurate calibration for the instrument [9, 27, 29, 30].

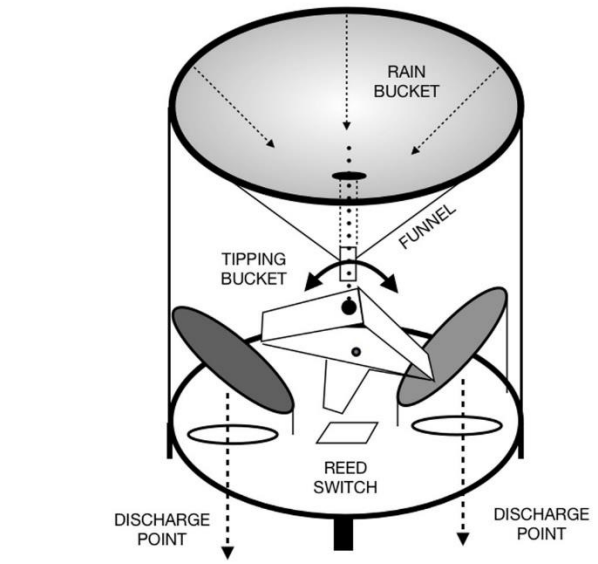

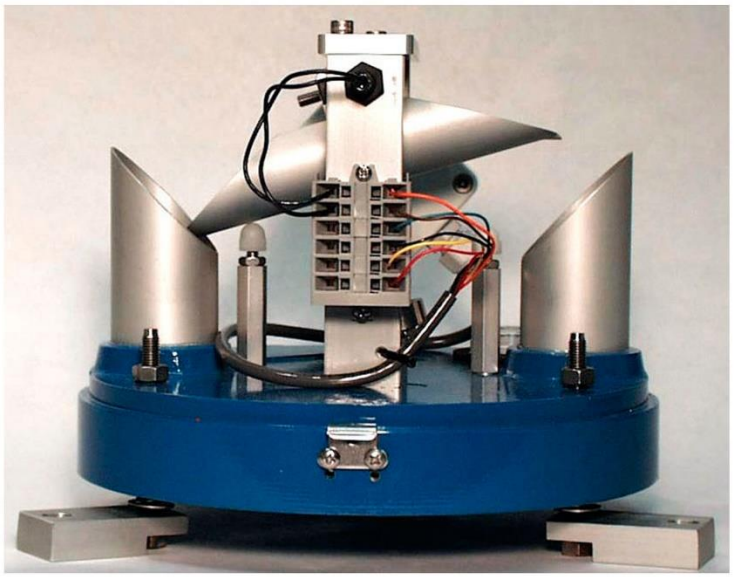

Figure 3: Typical sketch of Tipping bucket gauge [30]**.**

2.2.1.2 Weighing rain gauge

This weighted-type gauge uses the accumulation container to collect the rain (figure 4). It records the mass of accumulated water using different methods, for instance, a mechanical weighing rain gauges accumulate the rain in a container that attached with a spring. Then the movement transfers to a lever arm attached to a pen that records the weight of the collected rain. There are many benefits of using this gauge type among the tipping bucket gauges such as the estimation of the total rainfall event is measured accurately for high rainfall rates, nonetheless, it can measure other forms of precipitation (snow and hail).

Besides the benefits, there are other facts that can be considered as drawbacks. For instance, the prize of these gauges is relatively expensive besides it needs a continuous maintenance even more than the tipping bucket gauges [9, 25, 26].

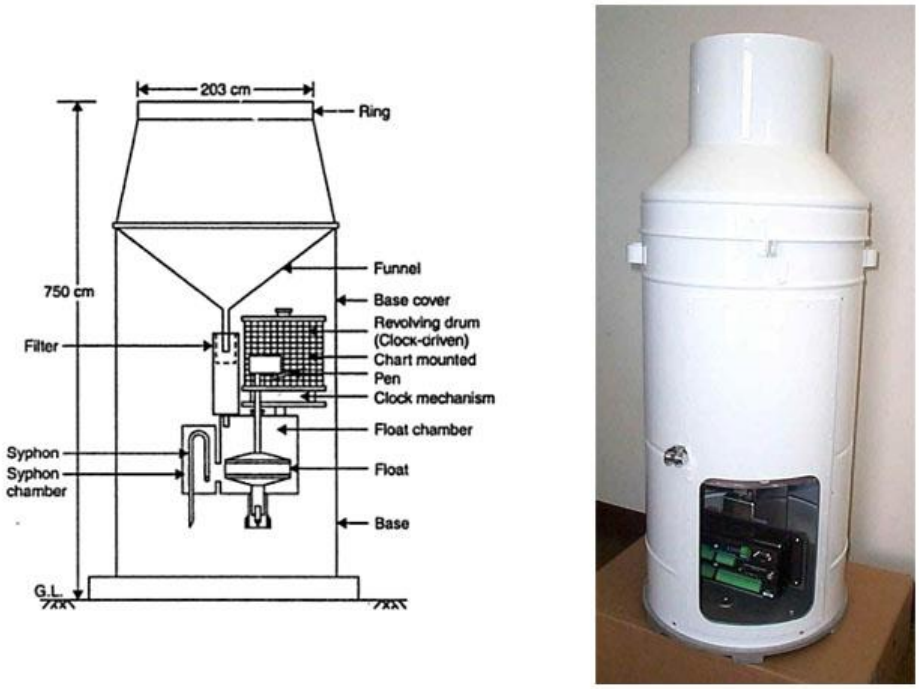

Figure 4: Typical Sketch of Weighting-type gauge [30]**.**

2.2.2 Disdrometers

A disdrometer is an instrument that is used to measure the velocity and the size of the water drops. It is reliant on an internal clock just like a tipping bucket (figure 5). It is recommended to perform a continuous calibration and adjustment of the disdrometer, as well as its clock, to ensure the clock will not drift with time.

The disdrometer has many significant features, for instance, it has the ability to determine the drop size distribution with time, using different methods. An impact disdrometer dictates assuming a value for the terminal velocity of drops, while in contrast, the image scan disdrometers determine the hydrometeor velocity individually besides the size and shape. Another feature of the disdrometer, their capability to measure the light rainfall rates which cannot measure by tipping buckets.

At most times, disdrometers required much more detailed rainfall information than any other rainfall measurement instrument. However, providing such additional information is not necessarily to provide an accurate rainfall measurement.

Eventually, for each gauge type, there are many advantages and disadvantages. However, the accuracy of rainfall measurement and analysis can be increased by utilizing some recommended approaches, such as utilization of multiple types of rain gauges distributed in a certain arrangement. Another recommended approach that enhances the amount of rainfall captured by rain gauges, is to use a collection of gauges and put them in a systematic order where the maximum distance between each one and another should be limited to one to two kilometers [9, 32]. This approach is efficient when the satellite or radar data were compared and tested with the ground observations in the particular area.

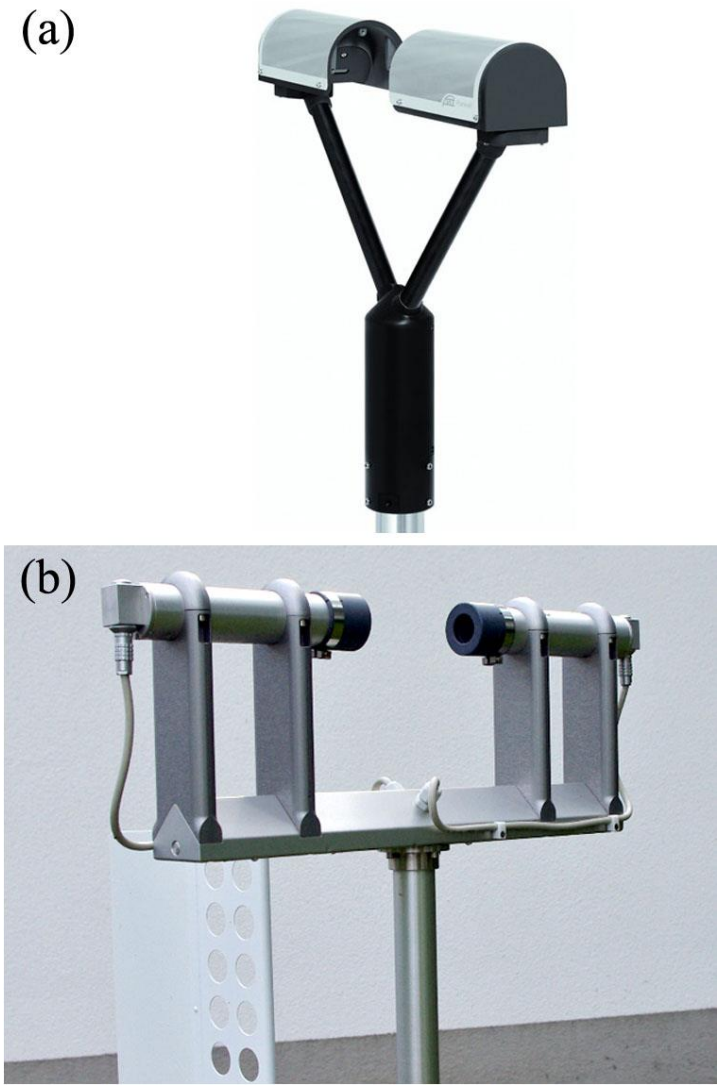

Figure 5: (a) Typical Sketch of Disdrometers and (b) optical Disdrometers [32]**.**

2.2.3 Radar measurements

The radar, as shown in figure 6, measures the precipitation indirectly by making use of backscattering of electromagnetic waves of the hydrometeors (water drops). The benefit here is the radar ability to monitor large areas with real-time high-resolution [33]. However, radar measurement has also many sources of errors, such as range-dependent systematic errors, mean-field systematic errors, and random errors. In addition, radar networks do not cover all parts of the world [21].

Figure 6: Ground weather radar [34]**.**

2.3 Satellite estimates

Utilization of multiple satellite sensors to measure the global precipitation in the past thirty years, increased significantly the special and temporal resolution of the precipitation detection [2, 9, 21, 25]. The formerly devoted satellite which is used for measuring the precipitation is Tropical Rainfall Measuring Mission (TRMM), which established in 1997 [19, 23, 24, 34]. The TRMM satellite was intended to measure the moderate to heavy Tropical Rainfall to produce a better understanding of the precipitation distribution around the globe as well as generating a near-real-time precipitation measures [19, 24, 34, 35].

Many free access products have been extensively studied and verified globally and regionally [21] and released for public use, for instance Precipitation Estimation from Remote Sensed Information Using Artificial Neural Networks (PERSIANN) [37], Climate Prediction Center (CPC) MORPHing technique (CMORPH) [38], PERSIANN Cloud Classification System (PERSIANN-CCS) [39], TRMM Multi-satellite Precipitation Analysis (TMPA) [40] and Global Satellite Mapping of Precipitation (GSMap) [41]. As a result, many researchers indicated that earth observing satellites perform well in measuring or estimating the precipitation rates and are also able to represent the spatiotemporal variations of precipitation for most parts of the world with high resolution [19 – 21].

Direct approaches and physically based algorithms have been achieved by prior quantitative and qualitative measurements of precipitation. The techniques utilized to derive the precipitation using the satellites progressed from Infrared-based (IR-based) and visible-based (VIS) methods throughout active (AMW) and passive (PMW) microwave approach to merging techniques.

2.3.1 Infrared techniques

Contemporary IR-based approaches which are used to estimate the precipitation by satellites have a lead of collecting a relatively excellent spatial resolution (near to 3 kilometers), high temporal resolution (15 minutes in case of Meteosat satellite) and, providing a considerable detection coverage [25]. The principle stands behind this estimation method is that huge vertical development of the cloud can be identified by detecting cold cloud tops. However, an indirect relationship is used to correlate the surface rainfall to the cold cloud tops, in fact, not all locations where have the heaviest surface rainfall lies beneath coldest clouds. Furthermore, the problem can be sophisticated, by view blocking of the precipitating cloud layer which caused by a system of multi-layer clouds [25].

An effective solution was introduced to support the metrological operations, by utilizing a different wavelength during several parts of the day which allow combining various algorithms together. However, this solution initiates a bias that Weakens the accuracy of those products and thus they are not capable of being used in climate-quality applications [25].

Furthermore, the IR methods facing a common problem, which the statistical relationship that connects the temperature of cloud tops with the actual ground rainfall is extremely reliant on the season and measurement position. Some efforts have been done to overcome this problem by introducing some effective operational methods, for instance, the Hydroestimator [42], the Autoestimator [43], the Convective/Stratiform (CST) technique [44] and, Global Precipitation Index (GPI) [45]. These methods minimized the spatiotemporal variability and performed well when it calibrated.

2.3.2 Active and Passive Microwave techniques

The satellites which utilize the microwave frequencies between Ku (10 GHz) and W (95 GHz) bands have a direct method to estimate precipitation, however, some satellite platforms have characteristics which allow using above or below the mentioned range of frequencies. Absorbing, scattering and emitting of the radiation by clouds and precipitation-sized particles are limited to the spectral range. In general, microwave satellites depending on two major estimation methods, Passive Microwave (PMW) and Active Microwave (AMW) technique.

The satellites which use the Passive Microwave (PMW) technique quantify the net thermal emission derived from the top of the atmosphere. The valuable feature of the interaction of the atmospheric constituents, for instance, precipitation particles, distributed clouds and water vapor with the microwave radiation resulted from surface emission, helped in performing the PMW techniques. One of the major factor affecting the spatial resolution of the sensors is the size of the antenna, specifically onboard low orbit satellites. Preserve a suitable antenna size made this type of satellites to have a relatively coarse spatial resolution (5 - 60 Kilometers). In addition, the temporal resolution is reduced for low Earth orbits because of limited fields of view.

On the other hand, the satellites which adopting the AMW technique calculate the power backscattered from a transmitted series of pulses. These satellites also known as spaceborne precipitation radars, the first satellite carrying Ku-band radar was released called TRMM precipitation radar which started to operate on 1997. The TRMM satellite has many applications and it was evaluated and reviewed extensively by many researchers such as [3, 9, 39, 45–48]. The world first W-band radar was carried by CloudSat satellite which

was launched in 2006, with a capability to measure or estimate the light rainfall rates as well as best identification of the cloud properties. The success of TRMM satellite era and the merged techniques were introduced, many approaches proposed to launch a new global satellite named as Global Precipitation Measurement (GPM), which has the ability to measure the precipitation around the globe precisely with the benefit of other constellation of some operating satellites.

2.4 Global Precipitation Measurement (GPM)

Global Precipitation Measurement (GPM) is an international collection of satellites grouped to provide next-generation measurements of global rain and snow at high spatiotemporal resolution (0.1^{o} x 0.1^{o} – half-hourly estimate). The constellation of the satellites consists of one main observatory satellite (figure 7) and around ten partner satellites (figure 8) [50]. The GPM Core Observatory satellite was launched by cooperation between National Aeronautics and Space Administration (NASA) and the Japanese Aerospace Exploration Agency (JAXA) on February 27, 2014, in non-sun-synchronous orbit with a microwave radiometer called GPM Microwave Imager (GMI) and a Dual-frequency Precipitation Radar (DPR). The GPM adopts a new technology and instruments, which level up the standards of precipitation measurements through combining the microwave and radar methods which proven its efficiency in TRMM era [21–23, 48]. The GPM mission aims to improve the knowledge about the global water and energy cycles, increase our capabilities to predict extreme events, and advance our understanding to get use the precipitation information and apply it directly in all science fields [51].

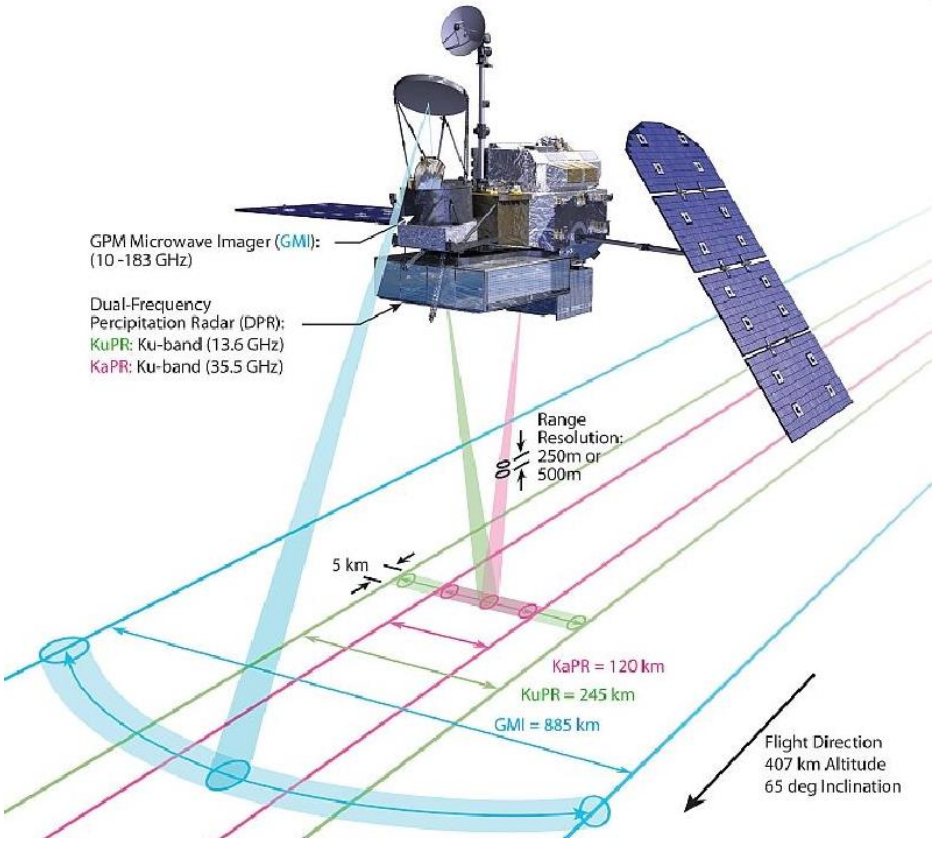

Figure 7: Schematic diagram of the area covered by the GPM core satellite (NASA website).

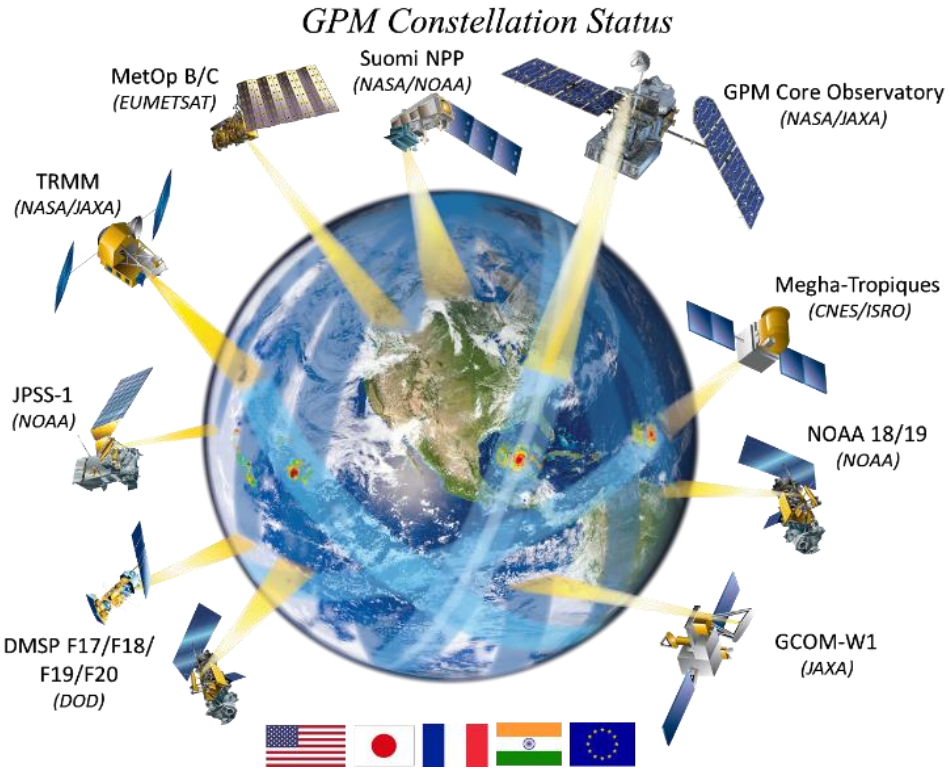

Figure 8: Satellites that frame the GPM Constellation (NASA website).

The GPM has many products and NASA named it under three categories or levels: Level-0, Level-1, and Level-3 (Table 1). The recommended product is level-3. This product is provided by the Day-1 Integrated Multi-satellitE Retrievals for GPM (IMERG) algorithm, which is designed to incorporate, merge, inter-calibrate all precipitation microwave estimate (MW), along with infrared satellite (IR) estimates, ground precipitation gauges, and all other precipitation estimators that were involved in Tropical Rainfall Measuring Mission (TRMM) satellite era [51, 52]. NASA provides three main IMERG products, near "Early" real time run products, "Late" run products, and "Final" run products.

Currently, comparison and evaluation of GPM IMERG Day-1 products with ground observation gauges are highly important because, if the product is proven to be adequate, then it will direct precipitation measurements to a new era, which will help scientists rely mainly on the satellite data which will increase the certainty of hydrometeorological applications. This study was conducted to evaluate the accuracy of GPM day-1 IMERG "Early, Late and final" run precipitation products using daily ground-based observations data as a reference in the whole regions of the Kingdom of Saudi Arabia over the period from October 1st, 2015 to April 30th, 2016.

Table 1: GPM levels and description.

Product level	Input Data	Distributed to user	Description
Level 0	-	No	Depacketized data by Application Process Identifier (APID).
Level 1A	Level 0	No	These data are managed as the master data in mission operation system. Main parameters: Sensor output value, satellite altitude and location information, sensor condition, conversion parameters.
Level 1B, 1C	Level 1A	No	Products created by geometric collection and processing. Main parameters: Received power, Brightness temperature.
Level 2	Level 1A, 1B, and 1C	Yes	Products containing various physical quantities related to precipitation. Main parameters: radar cross section on the earth surface, precipitation type, bright band altitude, attenuation-compensated radar reflectivity factor and precipitation intensity, spectral latent heating.
Level 3	Level 1 or Level 2	Yes	Products created by spatiotemporal statistical processing. Main parameter: Precipitation rate.

CHAPTER 3

STUDY AREA AND PRECIPITATION DATASETS

3.1 Study Area

This research will be applied on the whole kingdom of Saudi Arabia which covers the area located between 34°32'00"- 55°40'00" East and 32°15'00"- 16°22'00" North as shown in figure 9. In Saudi Arabia, there are thirteen administrative regions; Riyadh, Makkah, Madinah, Qassim, Asir, Tabuk, Hail, Jazan, Najran, Al-Baha, Al-Jouf, Eastern Region and The Northern Border region. Each region contains certain rain gauge stations. The rain gauge data was taken from the online resource of Ministry of Water and Electricity (MOWE) – Saudi Arabia for selected period of October 1st, 2015 to April 30th, 2016 [54]. Table 2 summarizes the rain gauges in Saudi Arabia.

The climate in Saudi Arabia is characterized by dry and extremely hot in the summer season and it is rainy warm in the winter season [15, 54]. During summer, the highest temperature varies from 45 C° up to 54 Co which occurs in the months of June and July; and in winter the temperature varies from 10 to 29C° [56]. The rain falls usually in the winter season, October to April [15]. However, the rain is not well distributed all over the regions of the Kingdom of Saudi Arabia.

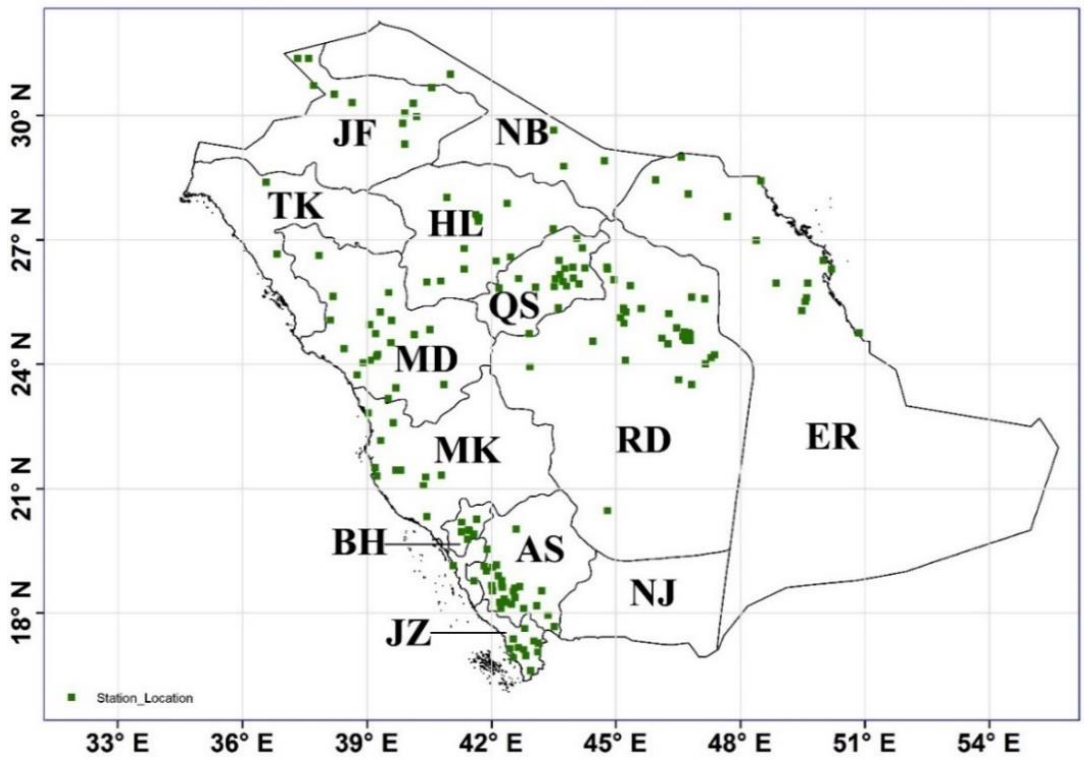

Figure 9: Map of Saudi Arabia and distribution rain-gauge stations.

Table 2: Saudi Arabia's regions and number of MOWE stations.

No	Region	Region ID	Number of Stations[1]
1	Riyadh	RD	38
2	Makkah	MK	14
3	Madinah	MD	21
4	Qassim	QS	21
5	Eastern Province	ER	16
6	Asir	AS	27
7	Tabuk	TK	2
8	Hail	HL	12
9	The Northern Border	NB	7
10	Jazan	JZ	13
11	Al Baha	BH	8
12	Al Jouf	JF	10
13	Najran	NJ	None[2]
		Total	189

[1] The number of stations is limited to the availability of the data.

[2] There was no available data for Najran region in the period of (October 1st, 2015 – April 30th, 2016).

Regional and local climate are exaggerated by large-scale atmospheric movement along with the features of the surface. Besides, atmospheric movement changes and variations are important aspects of the climate [14]. The features of the rainfall vary locally and regionally based on the patterns of the atmospheric circulation resulted by the El Niño Southern Oscillation (ENSO), North Atlantic Oscillation (NAO), and other variability patterns [10, 14, 15].

Generally, the rainy season in Saudi Arabia ranging from October to April [14 – 16], during this period the rain is described as scarce and irregular rain. When in the other months, nearly there is no precipitation observed in all region of Saudi Arabia except for the southwestern region [15]. The southwestern region suffers from a high spatial variation, due to the topography of the area (mountain area). The topographically driven convective rain in the southwestern region resulted in multi-rain events in this specific region of Saudi Arabia [11, 17, 18]. Overall, in desert areas, the mean annual precipitation is less than 100mm while in mountain areas it is ranging between 250-300mm [10, 11, 14].

3.2 Statistical Metrics

With the intention of assessing the performance of the GPM satellite precipitation measurements, six commonly used statistical measures were selected, which are generally grouped into three main sets on the basis of their indications [21–23, 56]. The first group is used to describe the bias and error of satellite data compared with rain gauge data which are Mean Error (ME), Root Mean Squared Error (RMSE) and Relative Bias (RB), while the second group contains only one statistical measurement, the Correlation Coefficient

(CC) which describes the agreement between rain gauge data and satellite estimates. The third group describes the contingency of satellite estimates using two statistical parameters: Probability of Detection (POD) and Critical Success Index (CSI). Tables 3 and 4 summarize the statistical metrics and their expressions, which were used to perform the comparisons between gauge data precipitation and satellite measurements.

Table 3: Statistical metrics used for comparison between gauge data and satellite data.

Statistical metrics	Equation	Used for
Mean Error (ME)	$\frac{1}{n}\sum_{i=1}^{n}(X_i - Y_i)$	Describe the bias and error of satellite data compare with rain gauge data
Root Mean Squared Error (RMSE)	$\sqrt{\frac{1}{n}\sum_{i=1}^{n}(X_i - Y_i)^2}$	
Relative Bias (RB)	$\frac{\frac{1}{n}\sum_{i=1}^{n}(X_i - Y_i)}{\sum_{i=1}^{n} Y_i}\ x\ 100\%$	
Correlation Coefficient (CC)	$\frac{\frac{1}{n}\sum_{i=1}^{n}(X_i - \bar{X})(Y_i - \bar{Y})}{\sigma_x \sigma_y}$	Describe the agreement of rain gauge data and satellite estimates
Probability of Detection (POD)	$\frac{P_{SG}}{P_{SG} + P_G}$	Describe the contingency of satellite estimates
Critical Success Index (CSI)	$\frac{P_{SG}}{P_{SG} + P_S + P_G}$	

Note: n denotes the number of measurement observations; X denotes satellite precipitation measurement; $\bar{X}$ denotes the mean of satellite precipitation measurements; Y denotes gauge precipitation measurement; $\bar{Y}$ denotes the mean of gauge precipitation measurements; σ_x represents standard deviation for satellite observations; σ_y represents standard deviation for gauge observations; P_{SG} represents the GPM satellite and rain-gauge detect a precipitation in a certain area; P_S represents the GPM satellite observe a precipitation in a certain area while the rain-gauge doesn't; P_G represents the rain-gauge observe a precipitation in a certain area but the GPM satellite doesn't.

Table 4: Contingency table to evaluate the detection of the satellite by measuring the POD and CSI parameters.

		Rain-gauge Observation	
		Yes	No
GPM product	Yes	P_{SG}	P_S
	No	P_G	-

3.3 Precipitation Datasets

3.3.1 Ground-based precipitation dataset

Rain gauges are considered globally as a reference of precipitation data as they provide a direct physical record of the precipitation at a given point. In this study, the daily rainfall data was collected from rain-gauge stations distribution all over Saudi Arabia via the online database service provided by the Ministry of Water and Electricity (MOWE). The database contains of 13 administrative regions, each region has many sub-region stations (Table 2). The collection of the data was determined according to the availability of the rainfall records during the investigated period from October 1st, 2015 to April 30th, 2016. The total number of observations recorded from the 189 rain-gauge stations is 1455. The spatial distribution of these rain-gauges are shown in figure 9. The rain gauges' network in Saudi Arabia is unequally distributed, as can be revealed from figure 9, which shows that it is densely spaced in the western (Madinah) and south-western region (Jazan and Asir), where the climate is wet, as well as in the middle region (Riyadh) where there is a dense population. However, eastern and northern regions have relatively sparse gauge stations. The variation of the data provided by MOWE is evaluated for each region through the descriptive statistical analysis, which is presented in table 5.

Table 5: Statistical parameters of the rainfall gauge data during the studied period (October 2015 to April 2016).

Region	Mean	Min.	Max	Standard Error	Median	Mode	Standard Deviation	Variance	Kurtosis	Skewness
Riyadh	9.26	0.1	57	0.68	5	2	11.23	126.00	4.81	2.23
Makkah	16.20	3	53	2.46	10.8	10	13.45	180.86	1.01	1.41
Madinah	11.67	0.4	54	1.17	9	6	11.20	125.35	4.68	2.06
Qassim	7.45	0.2	77	0.58	5.1	1	8.28	68.57	24.81	3.83
Eastern- Region	6.78	0.1	63	0.61	3.5	1	8.64	74.65	12.65	3.09
Asir	19.85	1.5	111	1.37	13	8	19.06	363.39	4.88	2.06
Tabuk	23.00	22	24	0.58	23	22	1.15	1.33	-6.00	0.00
Hail	4.71	1	22	0.40	4	4	3.69	13.58	9.27	2.59
Northern- Border	10.53	0.5	39.8	0.97	7	6	9.48	89.85	1.77	1.50
Jazan	16.46	1	96	1.52	10.3	2	17.17	294.93	4.29	1.81
Al Baha	17.52	1	119	1.64	13	3	18.28	334.31	8.40	2.43
Al Jouf	4.50	1	9	0.54	4.25	8	2.54	6.45	-1.12	0.19

3.3.2 Satellite-based precipitation dataset

The Integrated Multi-satellitE Retrievals for GPM (IMERG) is the Day-1 algorithm which is used to estimate the precipitation measured by a constellation of satellites. This algorithm has been used since the launch of the GPM Core Observatory and sustained to be used to estimate the amount of the precipitation. IMERG delivers a high spatiotemporal resolution precipitation products with 0.1^{o} x 0.1^{o} (longitude x latitude) – half-hourly estimate. IMERG provides three precipitation products based on latency and the need of the product which are: early run, late run, and final run products. The final run product is a post-real-time product provided with a latency of four months, while early and late run products are near-real-time, with a latency of 6 hours and 18 hours respectively. Table 6 summarizes the differences between the IMERG products and the previous/current satellite rainfall products, by comparing between the product resolution, latency, coverage, availability period and the spatiotemporal resolution. The GPM, three IMERG precipitation products, can be downloaded from NASA Precipitation Processing System (PPS), which uses FTP's servers to ease and manage the access of the GPM data. The servers used to download the Early run product is ftp://jsimpson.pps.eosdis.nasa.gov/NRTPUB/imerg/early/, for the Late run product is ftp://jsimpson.pps.eosdis.nasa.gov/NRTPUB/imerg/early/ and for the Final run product is ftp://jsimpson.pps.eosdis.nasa.gov/NRTPU/)

Table 6: Characteristics of the satellite precipitation products.

Satellite	Products	Resolution		Latency	Coverage	Availability Period	Correlated by gauges
		Spatial	Temporal				
GPM	IMERG - Early Run	0.1 degree	0.5-hourly	6 hours	65°N–65°S	March 2015–present	No
	IMERG - Late Run	0.1 degree	0.5-hourly	18 hours	65°N–65°S	March 2015–present	No
	IMERG - Final Run	0.1 degree	0.5-hourly	4 months	65°N–65°S	March 2014–present	Yes
TRMM	TMPA-3B42	0.25 degree	3-hourly	2 months	50°N–50°S	1997–April 2015	No
ECMWF	ERA-INTERIM	0.125 degree	daily	2 months	90°N–90°S	1979-present	No

CHAPTER 4

METHODOLOGY

To evaluate the IMERG products (early, late, and final), several main steps were carried out. Starting over with data processing, which contains two sub-steps, preparation of the ground measurements data and the GPM data processing and preparation. The subsequent step is data analysis, which contains three sub-steps, events determination using a VB. NET program, analysis of GPM converted files and Coordinates Matching Process (CMP) using VB.NET developed program. The last step is to compare the observed data by the satellite (GPM data) with the reference data (rain-gauge data) using widely used statistical measures. Figure 10 shows a general flowchart of the evaluation process.

4.1 Data Acquisition

4.1.1 Ground Measurements

As mentioned earlier, the data was collected from the website of the Ministry of Water and Electricity (MOWE) (figure 11). Next, the following steps were followed to prepare the data:

i. Starting date and End of the period were selected. Note that all dates are given in Hijri* calendar (*Hijri calendar is a lunar calendar consisting of 12 lunar months in a year of 354 or 355 days. A Hijri year is between 10 and 12 days shorter than a Gregorian year*)

ii. Territory and the gauge location were specified.

iii. Minimum precipitation amount was set to 1mm.

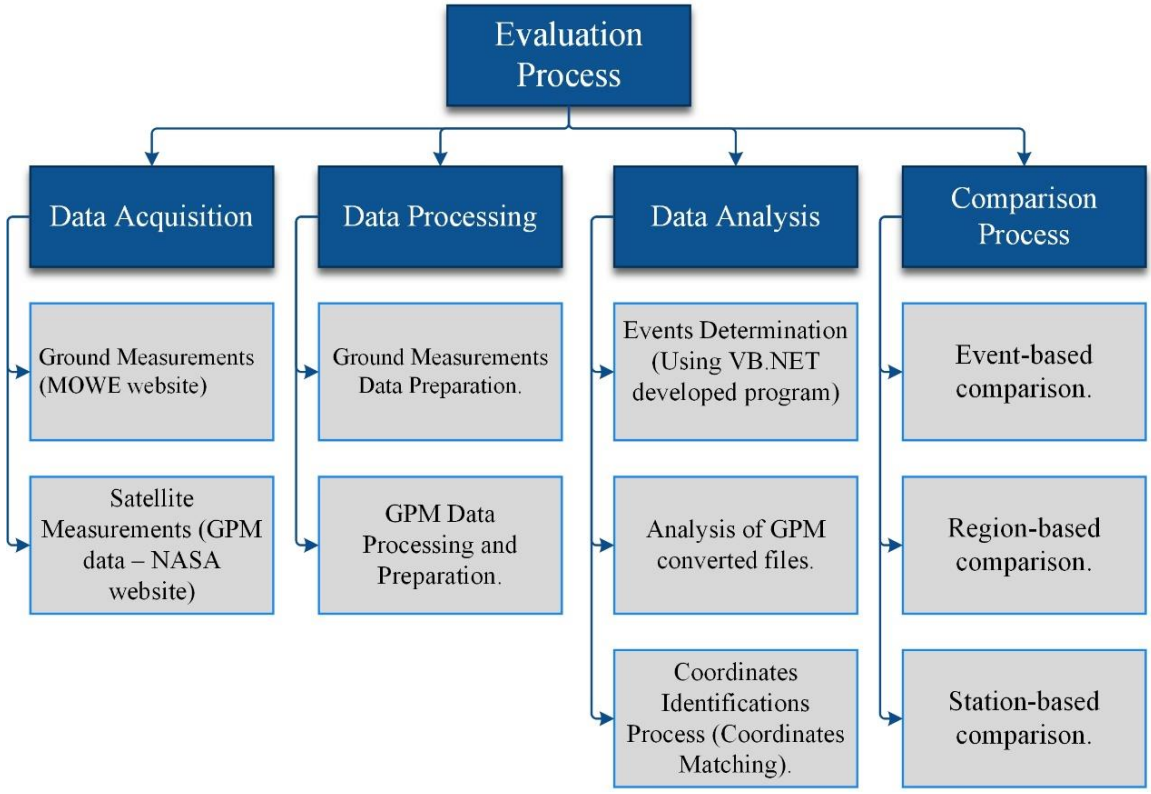

Figure 10: Flowchart of the evaluation process.

Figure 11: Online precipitation data web page provided by the Ministry of Water and Electricity website.

The Kingdom of Saudi Arabia has 13 administrative regions, the rainfall ground measurements were composed using the previously mentioned steps for the study period from 1st of October 2015 until 30th of April 2016. The number of rain-gauge stations, which have rainfall measurements during the selected period, found to be 189 stations. These stations recorded a total number of observations (rain records) 1455 rain records. Details about the station names which has measurements during the study period and their locations can be found in Appendix-A.

4.1.2 Satellite Measurements

Satellite measurements were collected from NASA website (GPM Data Downloads – Precipitation Measurements Mission) which is open for public use. With the purpose of downloading the GPM data from NASA servers, an application was used named as *CYBERDUCK* to ease access and download the data. The following steps were followed to download GPM data using *CYBERDUCK* (figure 12):

i. Open NASA servers using a special connection tool.

ii. User Name and Password were entered.

iii. The folder */DATA/IMERG* was selected and accessed.

iv. Files from October 2015 to April 2016 was downloaded directly to the platform.

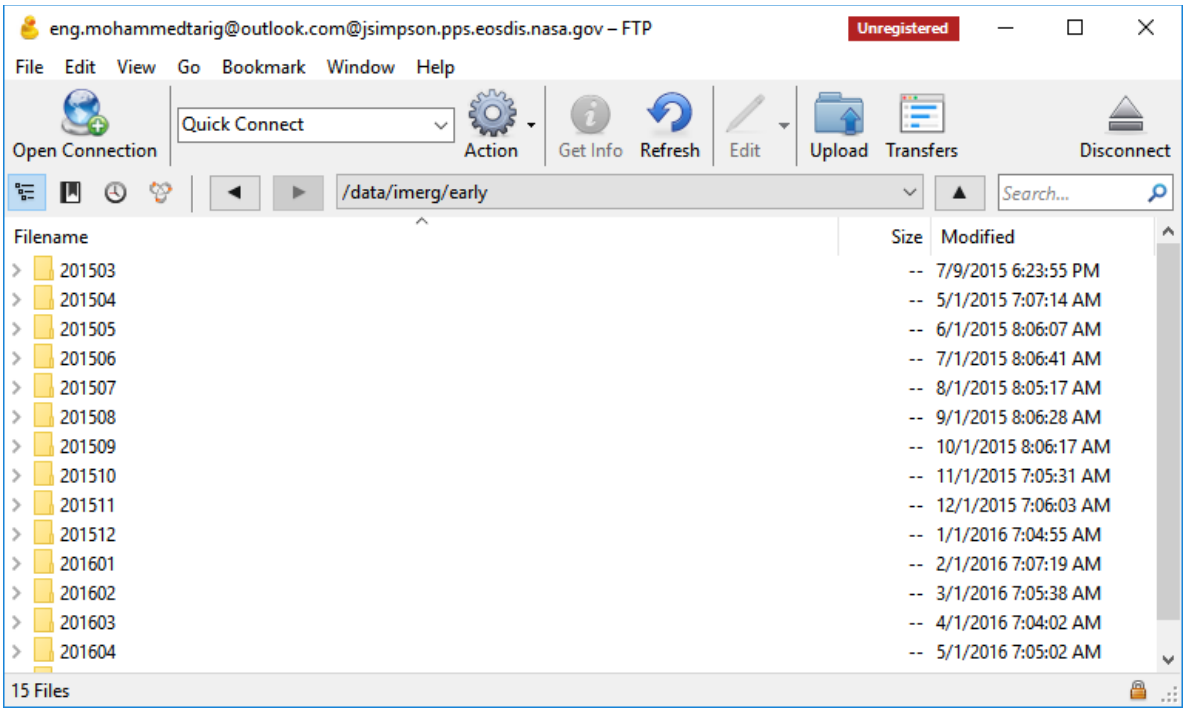

Figure 12: CYBERDUCK application interface.

4.2 Data Processing

4.2.1 Ground Measurements Data Preparation

The ground measurements data of the rain were download from the MOWE website in Arabic format and then it was translated from Arabic into English. Next, the rain-gauge station coordinates were determined either by personal contact or estimated using google earth merged with google maps. Following that, *GEOPLANER* website was used to determine the elevation (altitude) for each rain gauge station coordinate *(*http://www.geoplaner.com/*)*. The coordinates provided were in decimal degrees, so *UTM CONVERTER* program was used to convert the coordinates from decimals degree to UTM coordinates for each rain gauge station. Finally, a station-ID was assigned for each station which consists of two characters one to identify the territory and the other one to refer to the sequence in the database list.

4.2.2 GPM Data Preparation

GPM data was installed in the format of RT-H5 File, which is a representation of an HDF5 file. This type of file is unique technology suite that makes possible the management of extremely large and complex data collections. The GPM precipitation estimates cover all parts of the World and in order to carry out the comparison for Saudi Arabia, the data was extracted and converted to an ASCII format, using which is called R code. The R code can be modified to sum up the observed half-hourly precipitation to daily data or any time domain. In addition, the code is subjected to a constrains such setting the UTM zone, which is used to locate and extract the required data.

4.3 Data Analysis

4.3.1 Events Determination

The data, which was download from the MOWE website, contains more than 1450 records of rain-gauge observations that covers all parts of Saudi Arabia. The collected data contains too many information, i.e. precipitation amount, region/territory, gauge name, and coordinates. To determine the rainfall events occurred during the study period (from October 1st, 2015 to April 30th, 2016), RAINFALL_DATA_ANALYSIS program was developed using VB.Net programming language incorporated with MS Access as an internal database, to analyze all the data at once and specify the storm events according to the minimum number of occurrences (number of rain-gauge observations) which is set to 30 in this study. The following steps were followed to run the analysis using the developed program:

1. The event determination section was selected (figure 13). Minimum number of occurrence was chosen through numeric textbox (figure 14).

2. To perform the analysis process, *Calculate* button is pressed to save the results in internal database (figure 14).

Figure 13: Rainfall data analysis main interface.

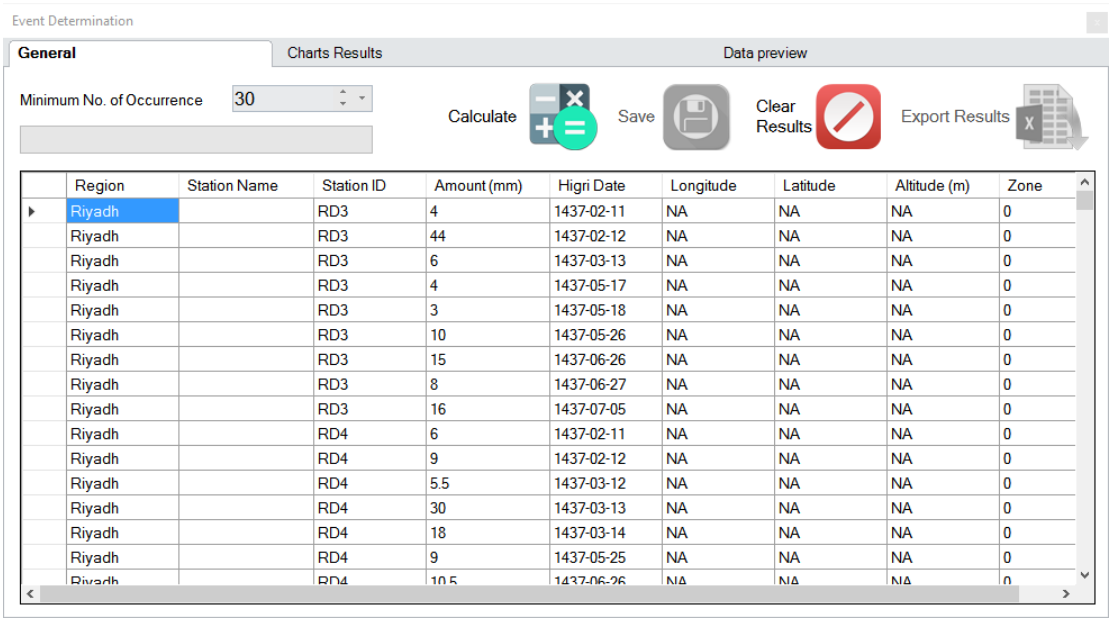

Region	Station Name	Station ID	Amount (mm)	Higri Date	Longitude	Latitude	Altitude (m)	Zone
Riyadh		RD3	4	1437-02-11	NA	NA	NA	0
Riyadh		RD3	44	1437-02-12	NA	NA	NA	0
Riyadh		RD3	6	1437-03-13	NA	NA	NA	0
Riyadh		RD3	4	1437-05-17	NA	NA	NA	0
Riyadh		RD3	3	1437-05-18	NA	NA	NA	0
Riyadh		RD3	10	1437-05-26	NA	NA	NA	0
Riyadh		RD3	15	1437-06-26	NA	NA	NA	0
Riyadh		RD3	8	1437-06-27	NA	NA	NA	0
Riyadh		RD3	16	1437-07-05	NA	NA	NA	0
Riyadh		RD4	6	1437-02-11	NA	NA	NA	0
Riyadh		RD4	9	1437-02-12	NA	NA	NA	0
Riyadh		RD4	5.5	1437-03-12	NA	NA	NA	0
Riyadh		RD4	30	1437-03-13	NA	NA	NA	0
Riyadh		RD4	18	1437-03-14	NA	NA	NA	0
Riyadh		RD4	9	1437-05-25	NA	NA	NA	0
Riyadh		RD4	10.5	1437-06-26	NA	NA	NA	0

Figure 14: Event determination input form.

The results generated by the program, after the second step, consist of two types of outputs:

a. *Charts*: to show the number of events detected in the database based on the event minimum observations and how many observations were determined for each event (figure 15).

b. *Tables:* here two tables will be generated. The first one shows the event date and the corresponding number of stations which has an observation in the same date. The second table represents the categorization for each event and detailed output which will be utilized in next analysis step (figure 16).

4.3.2 Analysis of GPM converted files

The metrics resulted from GPM data processing was analyzed by ensuring each date, as well as the UTM zones, contains the right coordinate intersections. Also, headers were added to the processed files to ease the searching process done by the RAINFALL_DATA_ANALYSIS program.

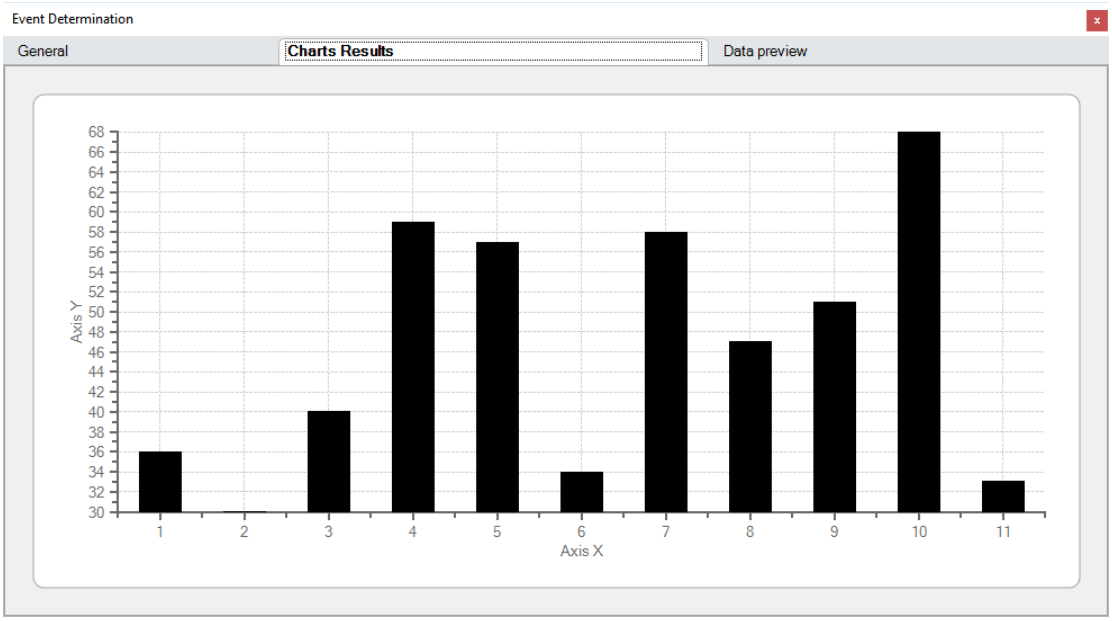

Figure 15: Events chart (Event ID in the x-axis and Number of Occurrences in the y-axis).

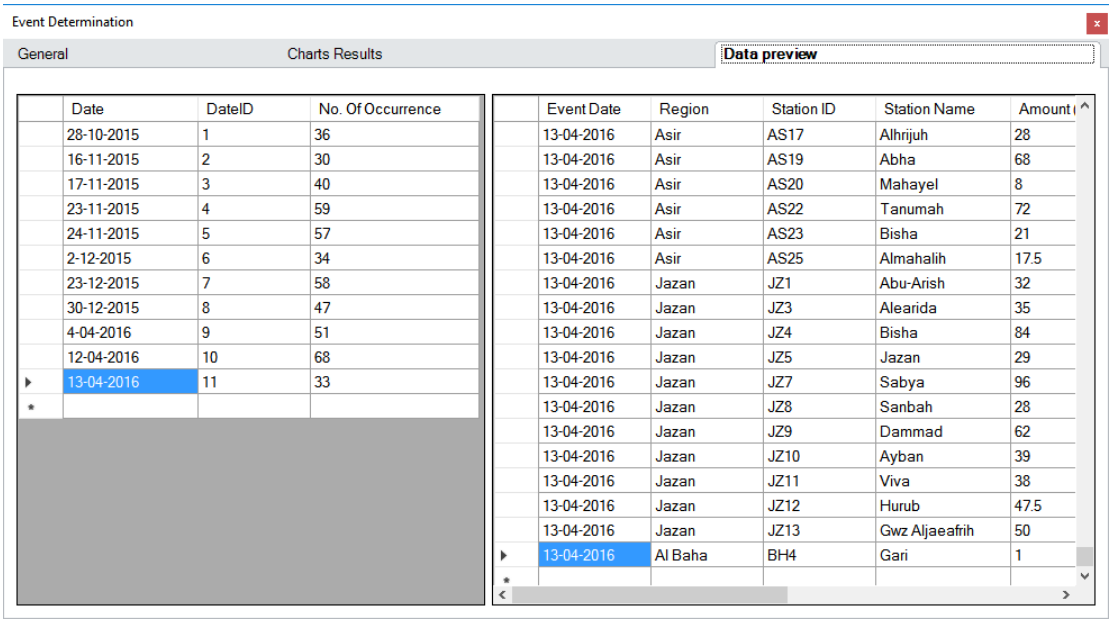

Date	DateID	No. Of Occurrence
28-10-2015	1	36
16-11-2015	2	30
17-11-2015	3	40
23-11-2015	4	59
24-11-2015	5	57
2-12-2015	6	34
23-12-2015	7	58
30-12-2015	8	47
4-04-2016	9	51
12-04-2016	10	68
13-04-2016	11	33

Event Date	Region	Station ID	Station Name	Amount
13-04-2016	Asir	AS17	Alhrijuh	28
13-04-2016	Asir	AS19	Abha	68
13-04-2016	Asir	AS20	Mahayel	8
13-04-2016	Asir	AS22	Tanumah	72
13-04-2016	Asir	AS23	Bisha	21
13-04-2016	Asir	AS25	Almahalih	17.5
13-04-2016	Jazan	JZ1	Abu-Arish	32
13-04-2016	Jazan	JZ3	Alearida	35
13-04-2016	Jazan	JZ4	Bisha	84
13-04-2016	Jazan	JZ5	Jazan	29
13-04-2016	Jazan	JZ7	Sabya	96
13-04-2016	Jazan	JZ8	Sanbah	28
13-04-2016	Jazan	JZ9	Dammad	62
13-04-2016	Jazan	JZ10	Ayban	39
13-04-2016	Jazan	JZ11	Viva	38
13-04-2016	Jazan	JZ12	Hurub	47.5
13-04-2016	Jazan	JZ13	Gwz Aljaeafrih	50
13-04-2016	Al Baha	BH4	Gari	1

Figure 16: Generated tables.

4.3.3 Coordinates Matching Process (CMP)

This process concerns with matching the location of the rain gauge station and the GPM measurement point. The CMP programmed using VB.Net programming language with incorporation of MS Access as an internal database. The main concept of the VB.net program is to perform the following procedure: (1) searching for every rain-gauge record in each event, using the record date and UTM station zone in order to select the right GPM file from the processed GPM data, then (2) reading the selected GPM file, and explore the UTM coordinates for each GPM intersection point to compare each intersection point with rain-gauge station location coordinates, finally (3) in case the intersection point lies inside the rectangular, as shown in figure 17, the corresponding rainfall measurements at that location is the match for the specified rain gauge station. A snapshot of the developed program devoted to do the above-mentioned steps is represented in figure 18.

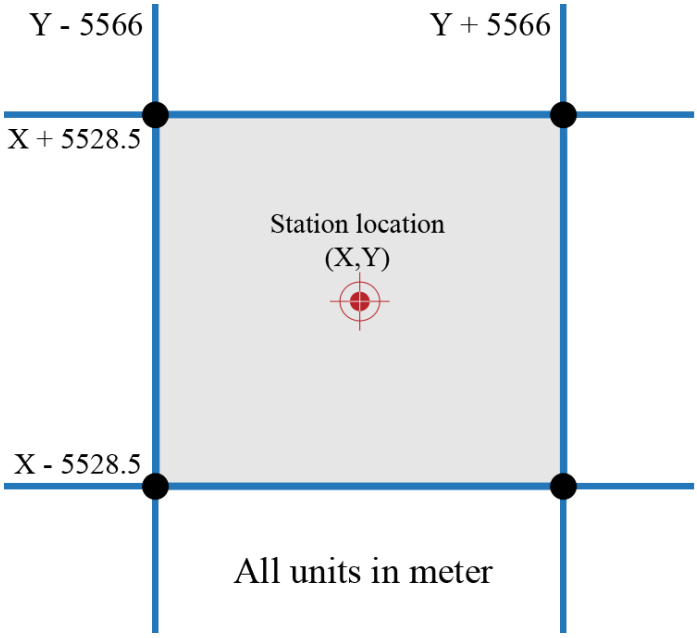

Figure 17: Coordinates matching process.

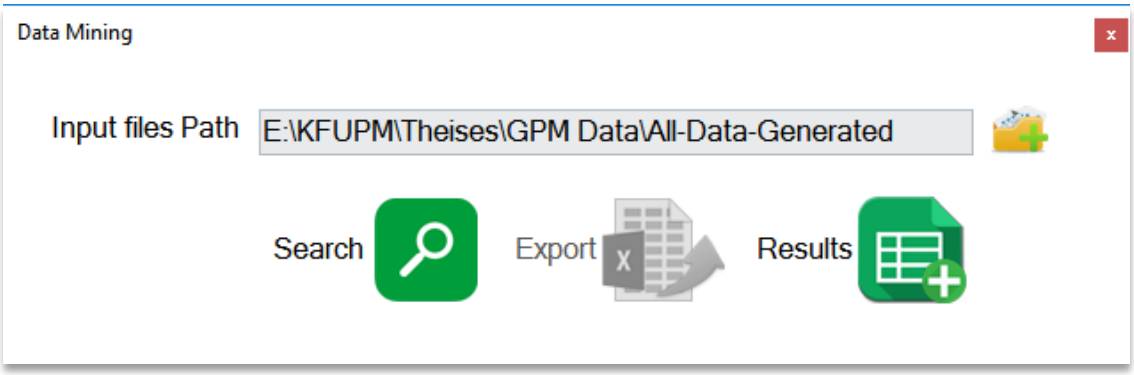

Figure 18: Data mining program interface.

4.4 Comparison Process

In this study, several statistical measures used to perform the comparisons between the ground (rain gauge) observations and the GPM measurements. Generally, there are three main comparisons or evaluations which have been conducted; event-based evaluation, region-based evaluation, and station-based evaluation. All the comparisons conducted for rainfall from October 2015 to April 2016 using IMERG products with $0.1^{o} \times 0.1^{o}$ spatial resolutions and daily temporal resolutions. The following paragraphs discuss the methods and assumptions adopted for the evaluations.

4.4.1 Region-based evaluation

The regional comparison conducted to evaluate the accuracy of the rainfall, which is detected by the GPM satellite for each sub-region versus the rainfall measured by the rain gauges within the same sub-region. The idea is to evaluate the overall accuracy of the measurements for the 12 administrative regions in Saudi Arabia.

4.4.2 Station-based evaluation

In this phase, the evaluation performed to represent the accuracy distribution of the performance of each rain gauge station. The idea is to deal with each rain gauge station independently, by collecting all rain record measured during the period by a single station. Then, a statistical analysis performed on these records.

4.4.3 Event-based evaluation

The event-based evaluation conducted based on selecting the largest events occurred during the study period (October 2015 to April 2016). Each day during the specified period, with a minimum of 30 rain gauge stations, where rainfall is recorded will be considered as an event. According to this assumption, eleven days were considered, resulted and tested as a major event.

CHAPTER 5

RESULTS AND DISCUSSION

With the purpose of assessing the accuracy of GPM day-1 IMERG "early, late and final" run precipitation products for each 0.1° × 0.1° grid cell that covered at least one rain gauge, the 189 rain gauges' precipitation records were used (figure 9). The 189 rain gauges recorded more than 1450 rain events during the rainy season (October 2015 to April 2016), which were used to calculate the mentioned statistical metrics. In addition, the assessment was carried out to perform the evaluation for three categories (region-based evaluation, station-based evaluation, and event-based evaluation) as mentioned in Chapter four.

5.1 Regional evaluation

GPM day-1 IMERG products have been evaluated regionally using statistical matrices over the whole Saudi Arabia during the study period from October 2015 to April 2016. The contingency of satellite precipitation estimates was evaluated through the Probability of Detection (POD) and the Critical Success Index (CSI) as shown in figure 19. The IMERG early product performed well in detecting the precipitation in most of Saudi Arabia's regions, however; only Makkah region suffers a relatively low detection (<0.6) compared with the other regions. In contrast, the IMERG late product showed a better performance of detecting the precipitation in all regions of Saudi Arabia including Makkah region (>0.7) as well. Moreover, the final run product, as can be revealed from figure 19, showed a powerful detection with almost 70% of Saudi Arabia has POD and CSI more than 0.9.

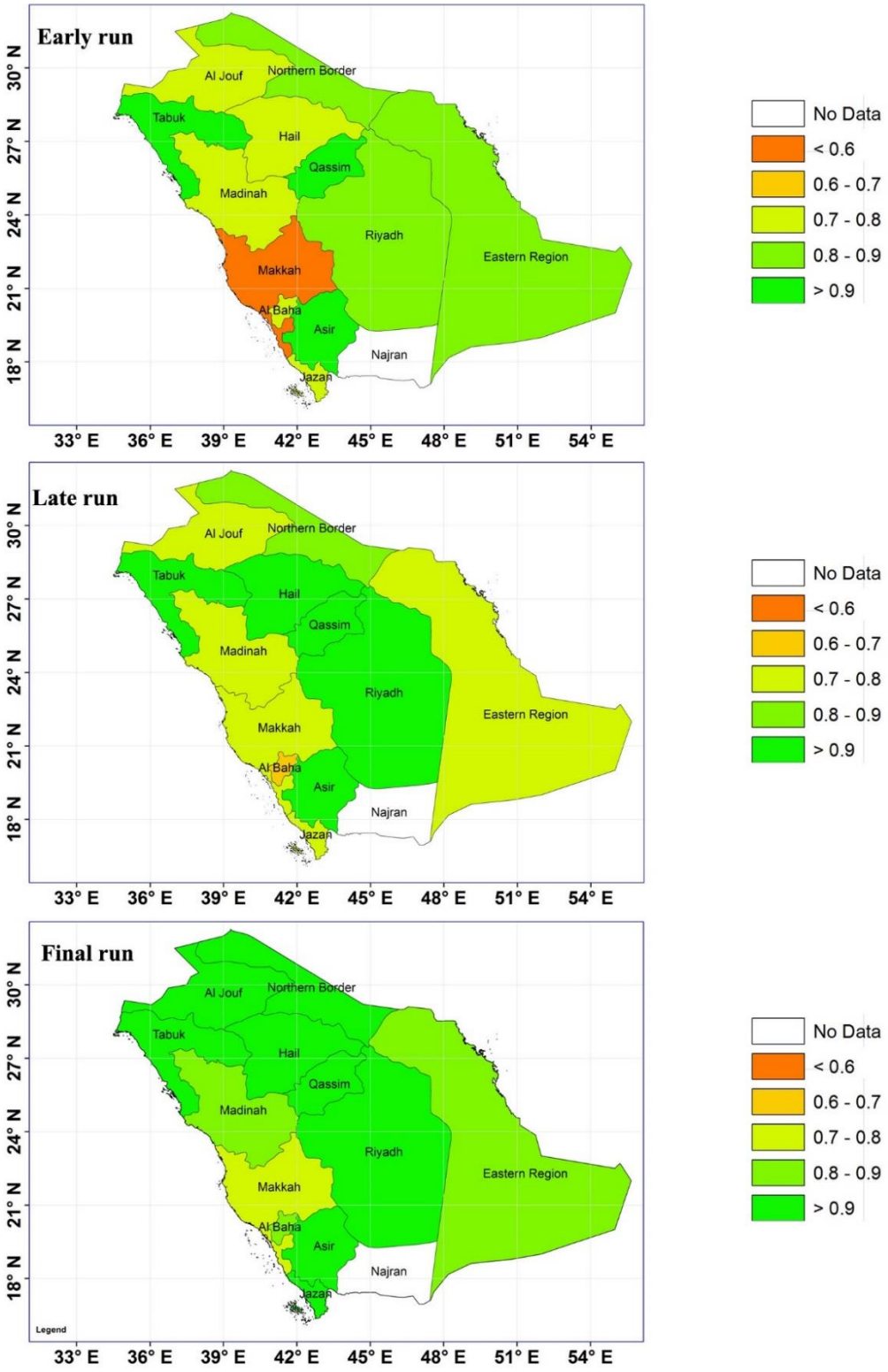

Figure 19: Regional spatial distribution of the Probability of Detection (POD) and Critical Success Index (CSI) estimation for IMERG early, late and final runs used in the regional evaluation.

The Mean Error (ME) was tested for all regions over the study period, and the ME values supported by the Relative Bias (RB) values are shown in figures 20 and 21, respectively. The figures indicate that for the IMERG early run product, the three regions Eastern Region, Madinah, and Qassim have a low ME and RB in detecting the precipitation with (±5 mm) and (±1%) respectively, which is considered a satisfactory performance in estimating the precipitation. While the satellite overestimates the precipitation over the Northern Border, Tabuk, Al-Jouf and Hail with an ME >10mm and RB >20%. On the other hand, the satellite measurements for the remaining regions, Jazan, Asir, Al-Baha, Makkah, and Riyadh, underestimates the precipitation with more than -10mm and -5%, for the ME and RB, respectively. Conversely, the IMERG late run product showed the same performance for most of the regions except for Asir and Makkah, which showed a significant enhancement by lowering the mean error to (±5 mm) and the relative bias to (±1 mm). In contrast, the IMERG final run product showed a substantial improvement all over Saudi Arabia. The figures reveal that the final satellite product has low values of ME and RB compared to the other products. In general, the results indicate that approximately 70% of all the regions of Saudi Arabia have an ME of ±5 mm and RB of ±1 mm.

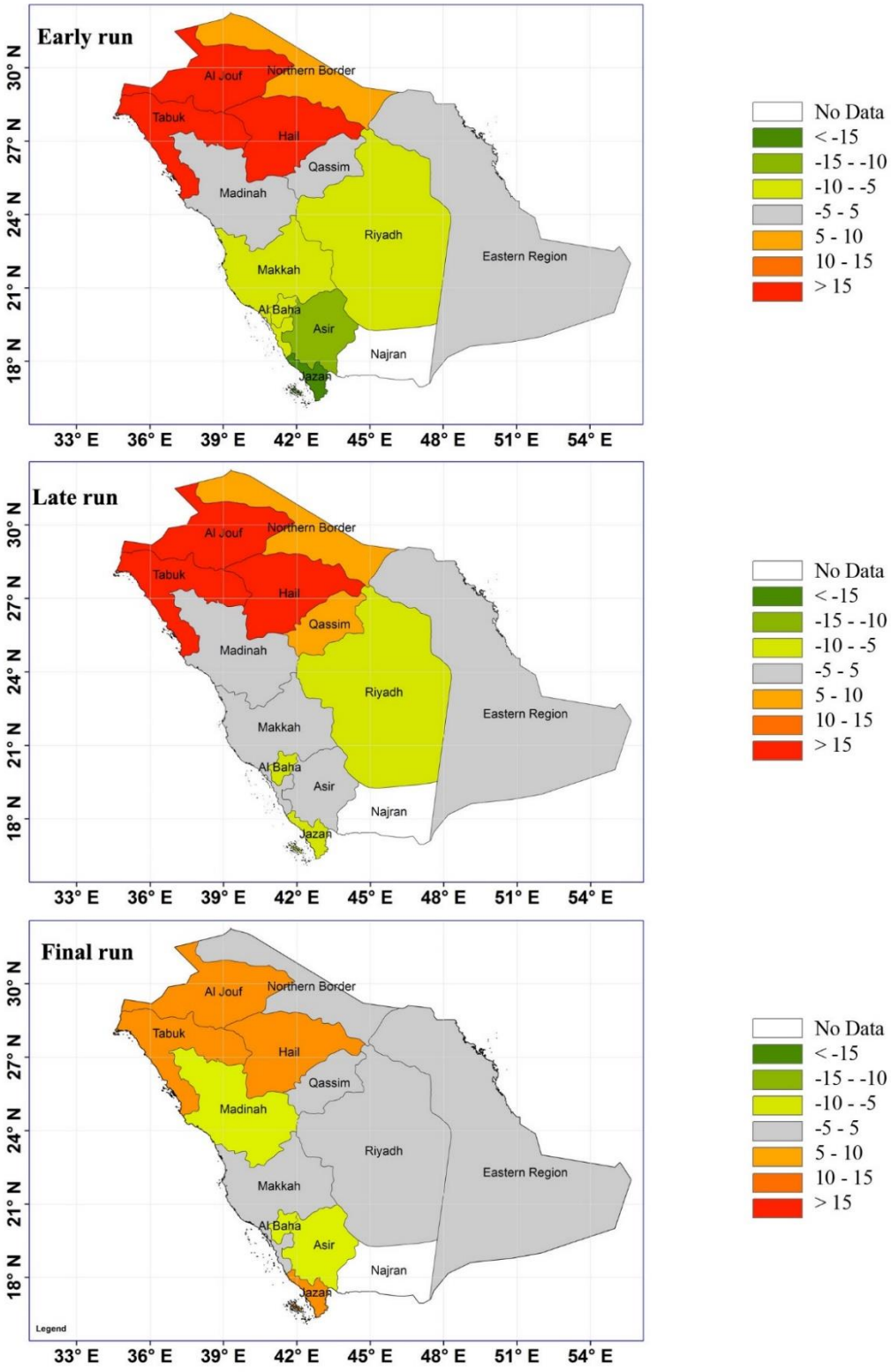

Figure 20: Regional spatial distribution of the Mean Error (ME) estimation for IMERG early, late and final runs used in the regional evaluation.

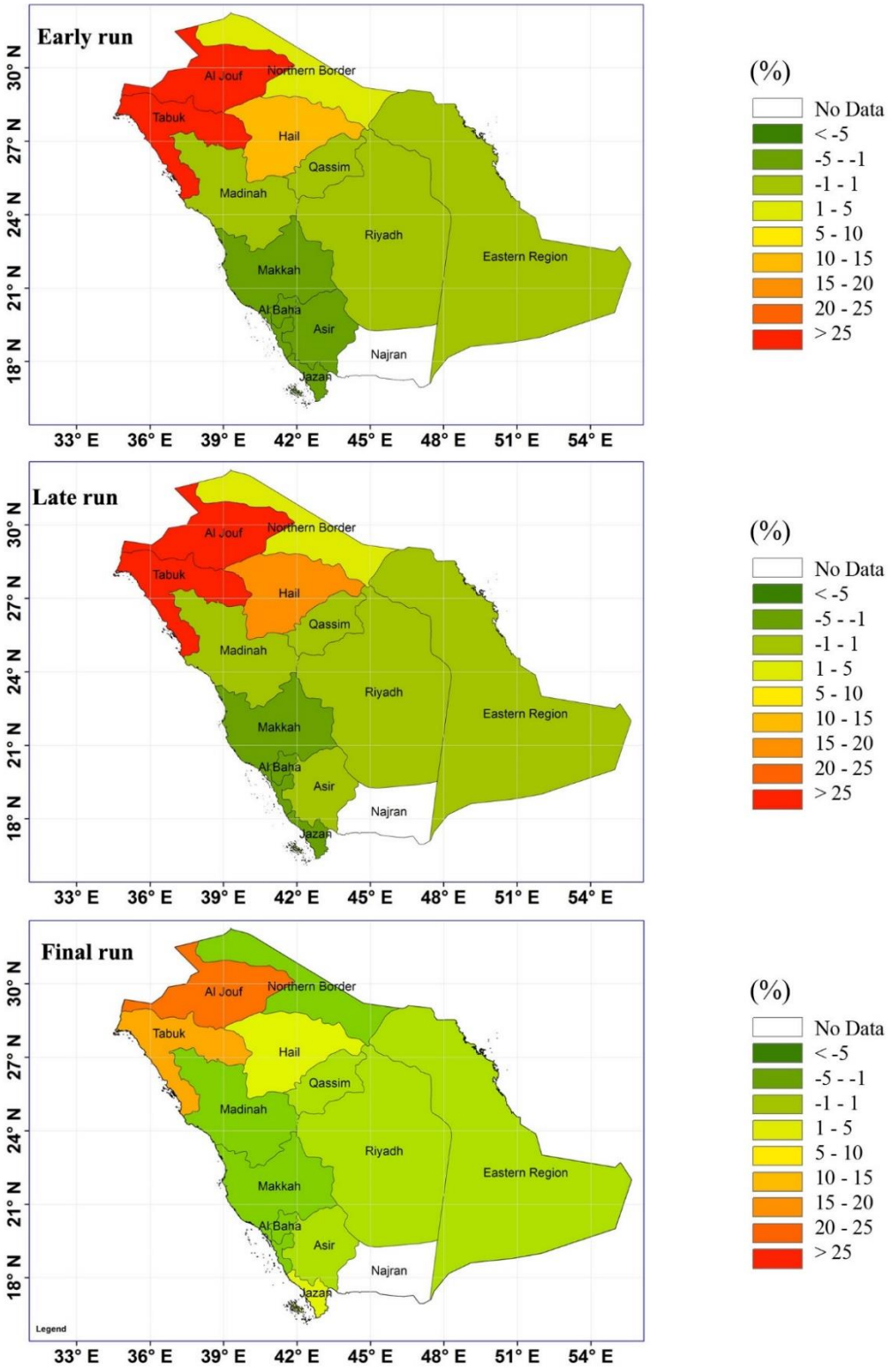

Figure 21: Regional spatial distribution of the Relative Bias (RB) estimation for IMERG early, late and final runs used in the regional evaluation.

Nevertheless, The Root Mean Squared Error (RMSE) results of the IMERG early run product showed a relatively low error for Riyadh and Eastern Region with less than 10mm, which indicates that the satellite has good measures over these regions (see figure 22). While the Northern Border and Makkah have a moderate RMSE (20mm), the other regions (Tabuk, Hail, Al-Jouf, Madinah, Qassim, and Al-Baha) have high values of RMSE (more than 30mm) indicating poor satellite estimation. The IMERG late run product exhibited a considerable improvement of RMSE which was reduced from 40mm to 20mm for the regions of Asir and Jazan. On the other hand, the IMERG final run product showed low RMSE values indicating high accuracy in precipitation estimates. The results indicate that all regions have RMSE values less than 15 mm, except for Hail, Madinah, and Asir where the RMSE ranges between 15-30mm.

The study also investigated the correlation between the satellite estimates and the rainfall gauge data through the Correlation Coefficient (CC). The results indicate that Riyadh, Tabuk, Jazan, Al-Jouf and Hail regions have a relatively high CC values (more than 0.5), for the IMERG early run product. While for the late run product the CC for the same regions as well as Asir and Qassim regions were enhanced with a considerable value (Avg. 12%) as shown in figure 23. On the other hand, the Northern Border, Eastern region, Makkah, Al-Baha and Madinah regions showed a relatively low correlation between the rainfall gauge data and the satellite estimates based on the early and the late runs. In contrast, the final run product, as shown in figure 23c, indicates high correlation between the rainfall gauge data and the satellite estimates. The results showed that the CC values for almost all Saudi Arabia’s regions were more than 0.5, leaving behind only Al Baha, Makkah and, Madinah with CC ranging from (0.1 – 0.2).

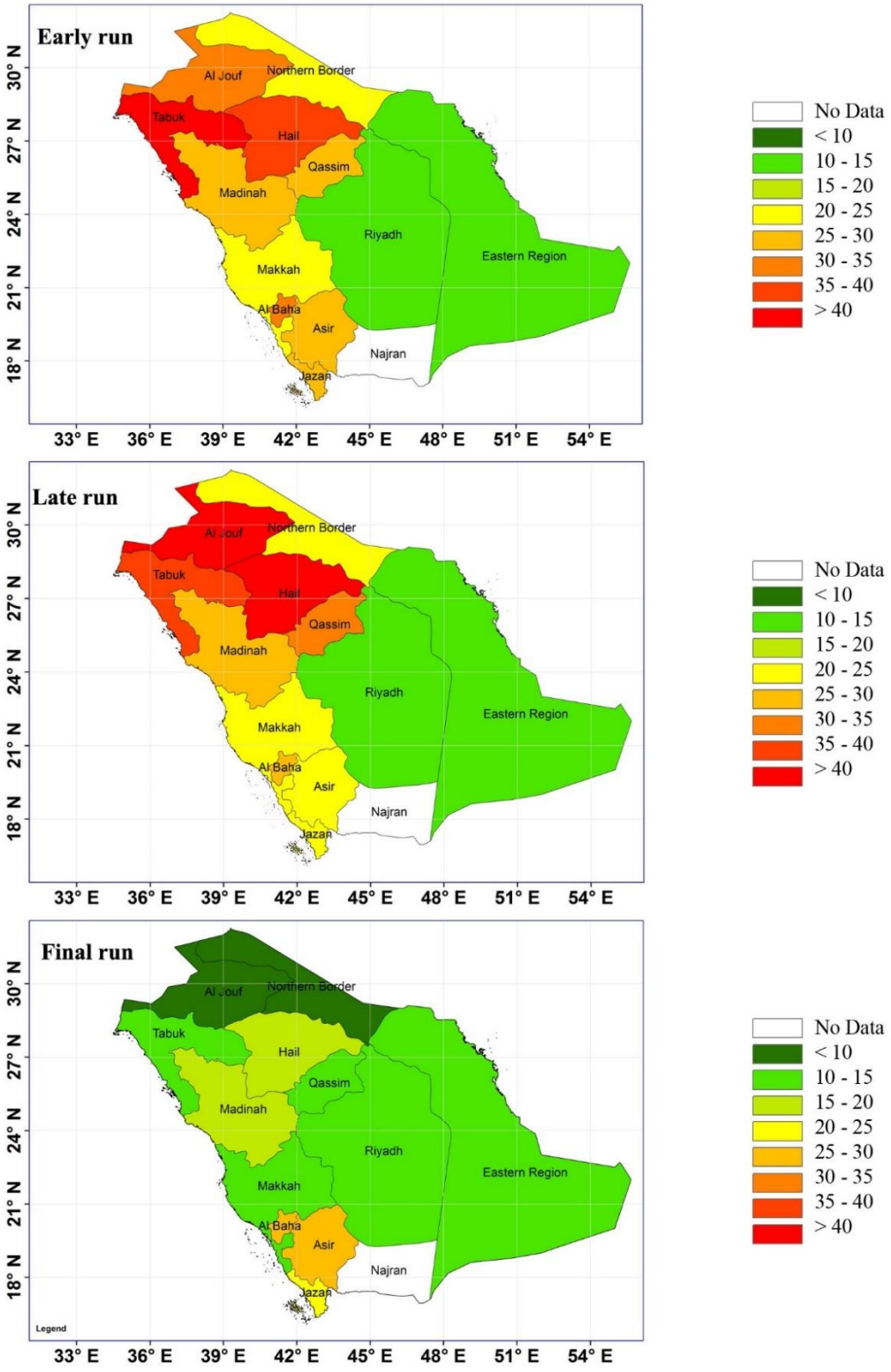

Figure 22: Regional spatial distribution of the Root Mean Squire Error (RMSE) estimation for IMERG early, late and final runs used in the regional evaluation.

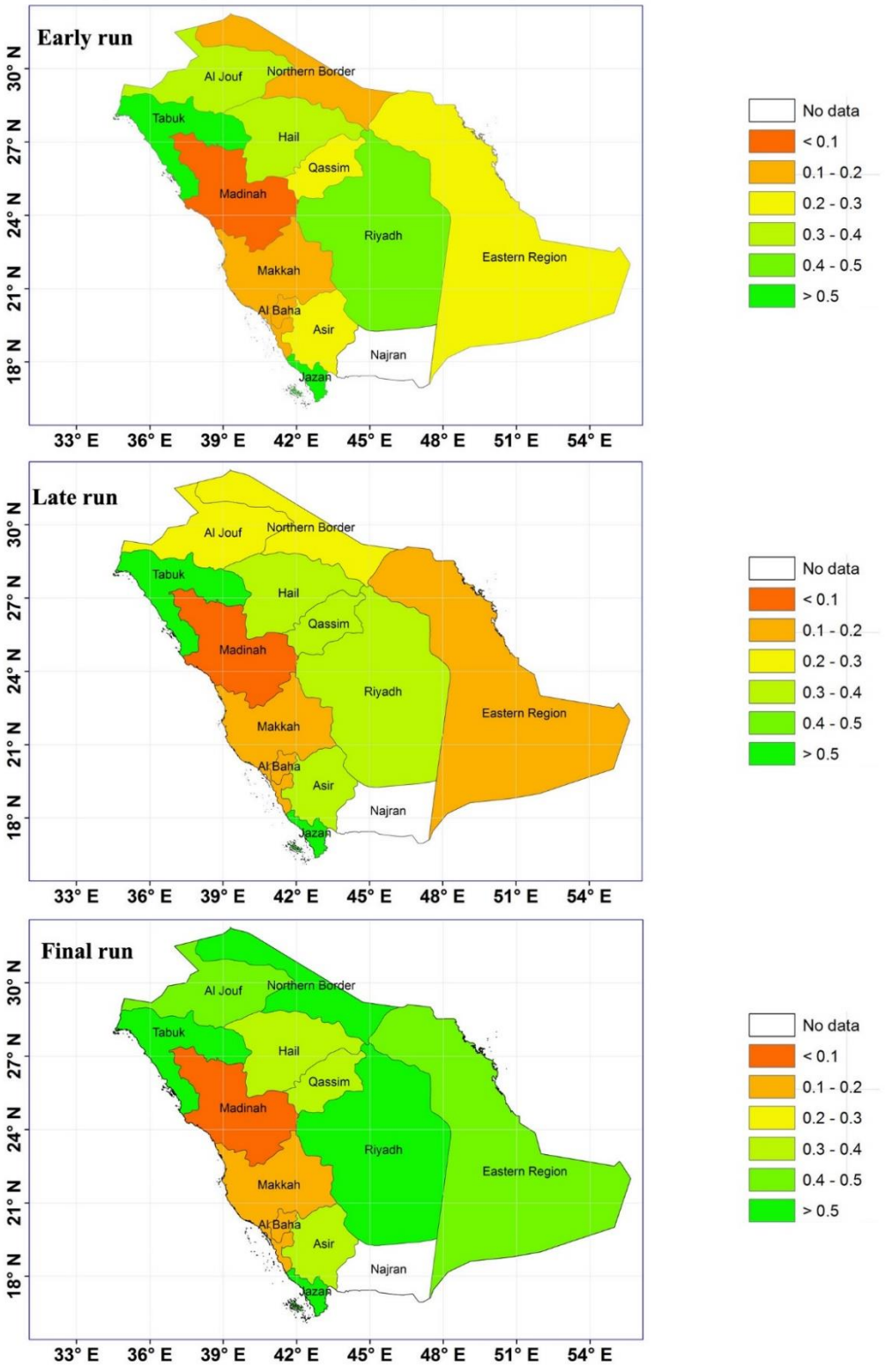

Figure 23: Regional spatial distribution of the Correlation Coefficient (CC) estimation for IMERG early, late and final runs used in the regional evaluation.

5.2 Station-based evaluation

This evaluation conducted by comparing the rainfall data of individual rain gauge station with the GPM estimates. For this purpose, the statistical matrices (table 3) were calculated and interpolated using GIS IDW tool in order to investigate the variation of each statistical parameter over the whole Saudi Arabia. The result represents the spatial variation depending on the accuracy of the individual station measurements.

The first statistical parameters group represents the Probability of Detection (POD) and Critical Success Index (CSI). The evaluation of the satellite estimates using these statistical parameters for IMERG early run product, as shown in figure 24, reveals high POD values (more than 0.8) except for the south-eastern part which was ranging from 0.5 to 0.7. For the south-eastern part, which contains the desert of Rub' al-Khali, a low POD and CSI were observed which indicates poor satellite-based precipitation estimates. Also, the results indicate that a small portion of the western part has low detection of the precipitation events. The results were improved through the IMERG late run product to reach POD and CSI values more than 0.75 for low detection areas. For the final run product, the figures revealed a substantial detection of the precipitation for all parts of Saudi Arabia with more than 0.85 POD and CSI (figure 24 and 25). Once again, the IMERG final product proven its capability to have the most accurate precipitation estimates in compare with the other IMERG products.

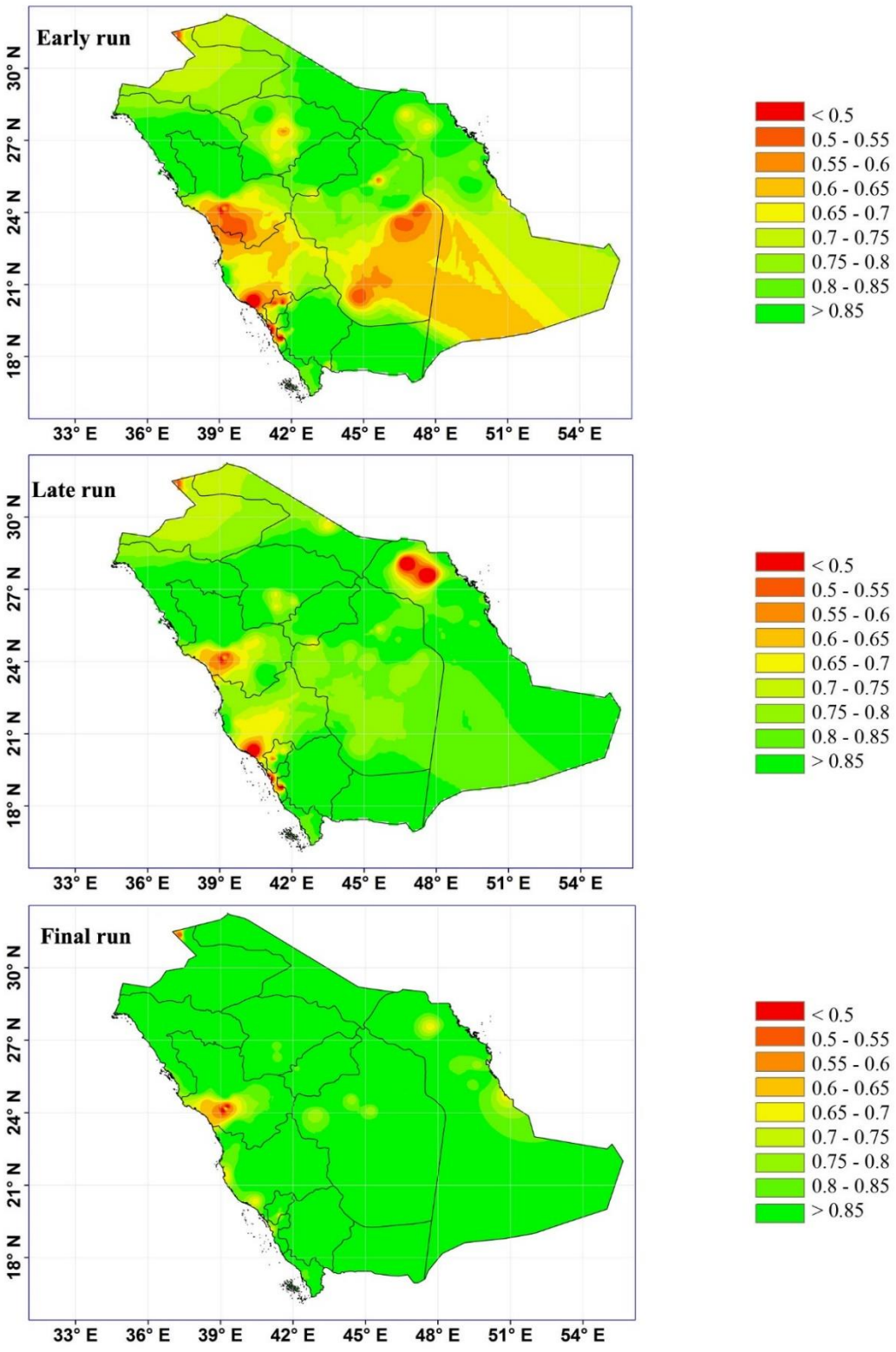

Figure 24: Spatial distribution of the Probability of Detection (POD) estimation for IMERG early, late and final runs used in the station-based evaluation.

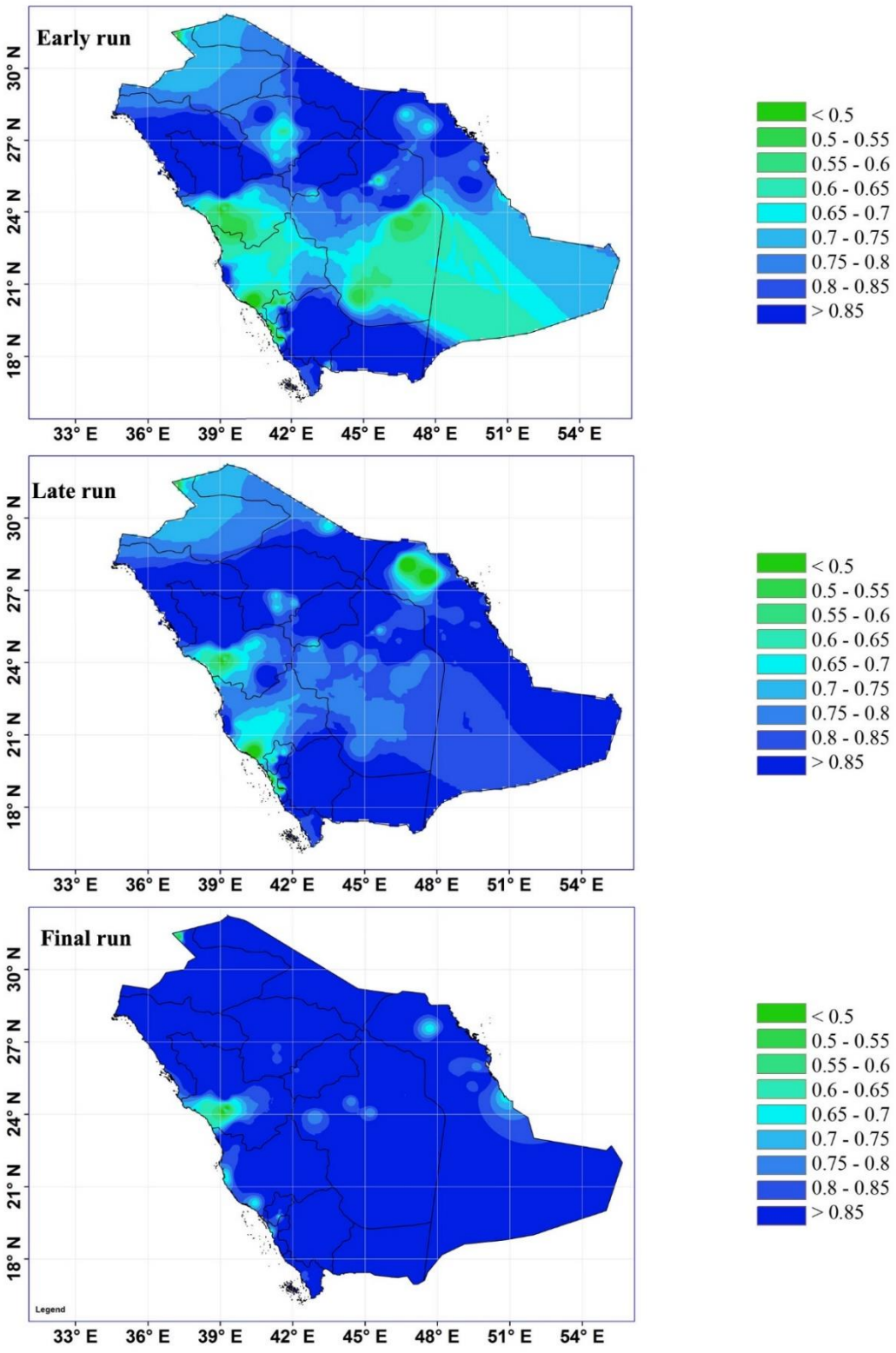

Figure 25: Spatial distribution of the Critical Success Index (CSI) estimation for IMERG early run, late and final runs used in the station-based evaluation.

The second group of the statistical parameters used for the station-based evaluation are: Mean Error (ME), Root Mean Squared Error (RMSE) and Relative Bias (RB). Starting with the ME, the results, as shown in figure 26, revealed a high error in the estimates (more than 15mm) for the stations located in the northern and the north-western part of Saudi Arabia for IMERG early run product, while the middle and the southern part have moderate values of the mean error (less than10mm). The eastern part and portion of the western part have a very low ME values (±5 mm) indicating better estimate compared to the other parts of Saudi Arabia. Conversely, the ME of the late run product estimates decreased in the southern part as well as the western part to the low ME (±5 mm), however; the northern and the middle part of Saudi Arabia suffer a high mean error with more than (10mm). On the other hand, the final run product showed a significant improvement over more than 80% of Saudi Arabia's parts (figure 26c) with only 5 mm error for most of the stations. Moreover, RMSE and the RB supporting the ME results as shown in figures 27 and 28, respectively. The results showed the same trend of the ME results which gives the eastern and the western part the precedence to have the perfect satellite estimation in compare with the ground observations for an early run and late run products. However, the IMERG final run product proven its efficiency for estimating the precipitation with very low errors and bias in compare with the other IMERG products.

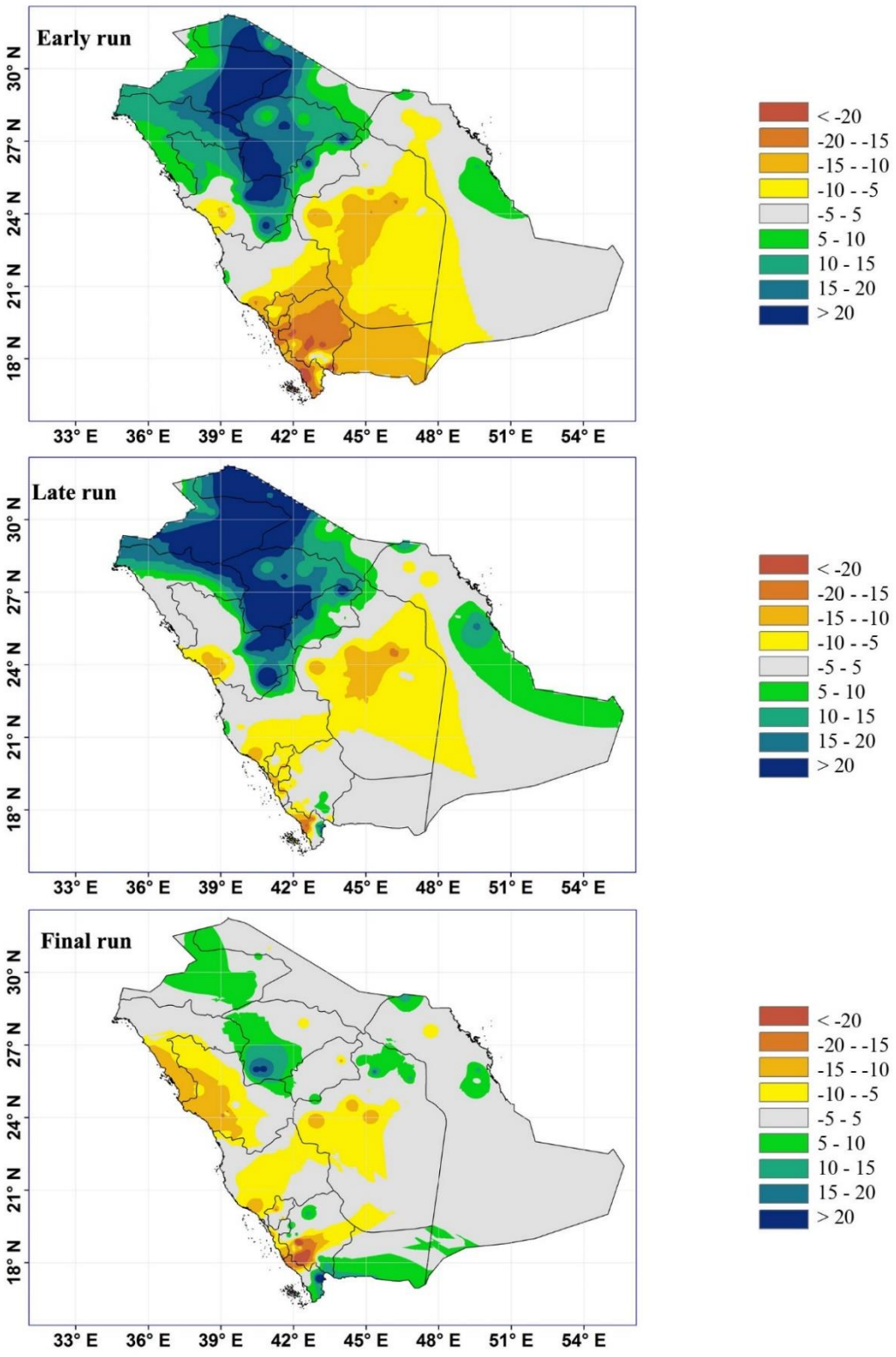

Figure 26: Spatial distribution of the Mean Error (ME) estimation for IMERG early, late, and final runs used in the station-based evaluation.

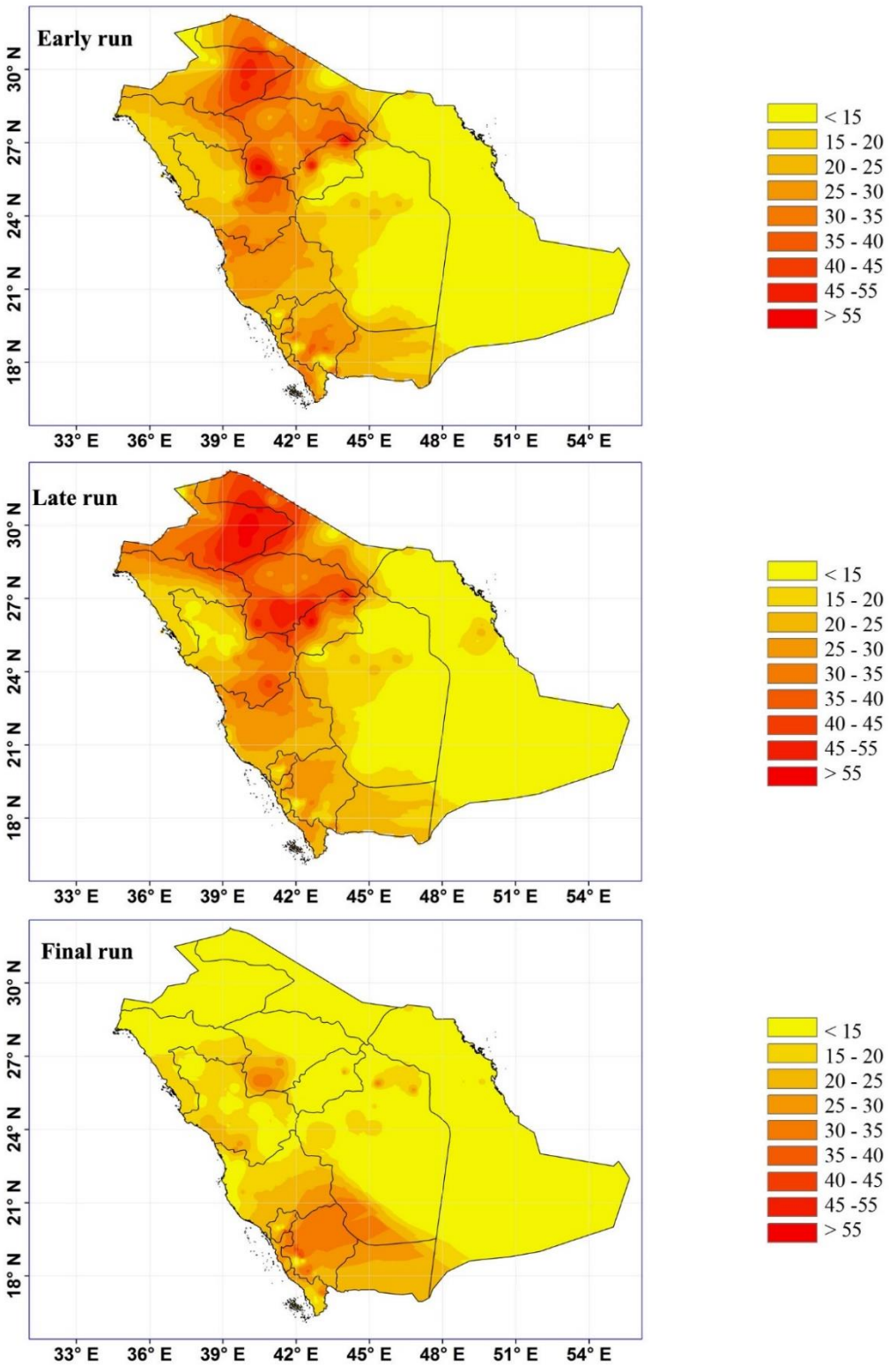

Figure 27: Spatial distribution of the Root Mean Squire Error (RMSE) estimation for IMERG early, late, and final runs used in the station-based evaluation.

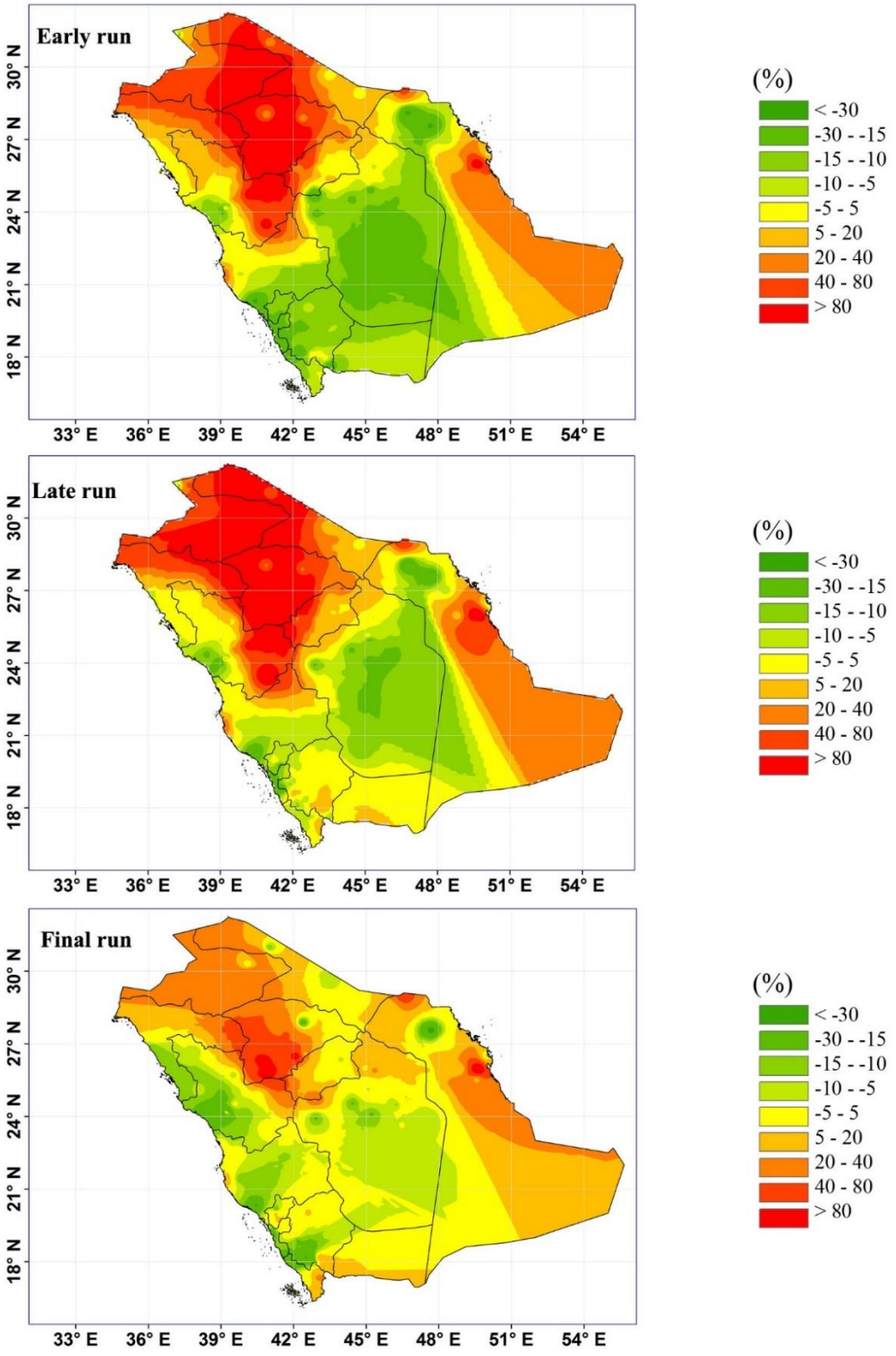

Figure 28: Spatial distribution of the Relative Bias (RB) estimation for IMERG early, late and final runs used in the station-based evaluation.

The Correlation Coefficient (CC) between the rainfall gauge stations and the GPM measurements for the different products are presented graphically as shown in figure 29. The figure showed that for the early run product, figure 29a, the southern, northern and the upper part of the eastern region of Saudi Arabia had a good correlation between the satellite data set and the rain gauge observations. The results enhanced significantly for the late run (figure 29b) and final run (figure 29c) products for two areas namely the southern and eastern regions. However; in the northern part, the CC was reduced in the late run due to high bias in estimation of the precipitation as mentioned in the first group evaluation. Nevertheless, the CC for the northern region show some improvement in the final run product (figure 29c). For the other regions of Saudi Arabia, high variations observed which could be related to the heterogeneity of the rainfall distribution and the variation of the topography of the land especially the middle and the western parts of the kingdom.

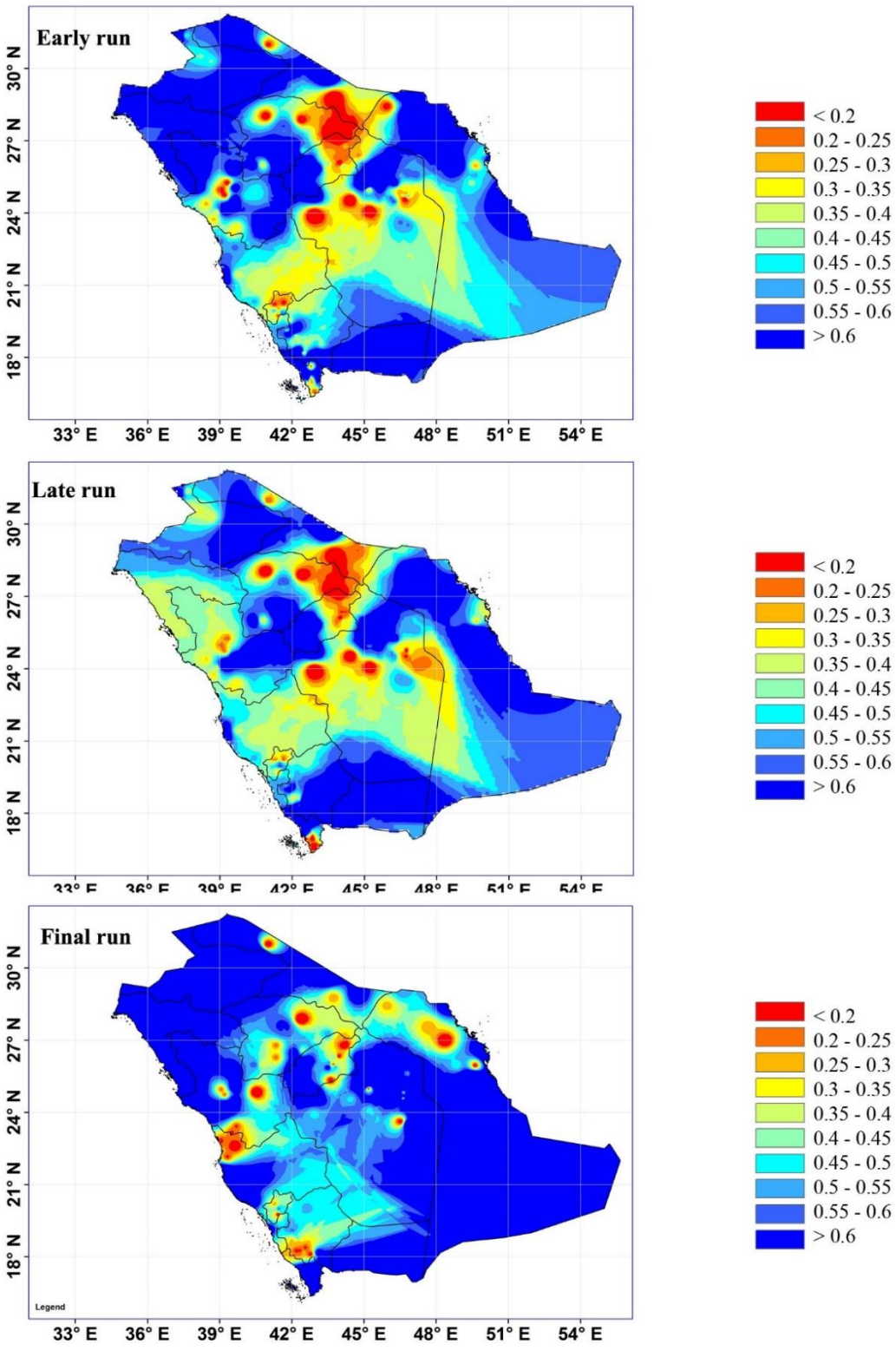

Figure 29: Spatial distribution of the Correlation Coefficient (CC) estimation for IMERG early, late and final runs used in the station-based evaluation.

5.3 Event-based evaluation

The event-based evaluation was conducted based on selecting the largest events occurred during the study period (October 2015 to April 2016) and compare them with the satellite data sets. The events were considered major or large event when the number of stations observed a precipitation exceeded 30 stations (rain storm covers more than 40% of the total Saudi Arabia's land) at the same date. According to this assumption, eleven-days were considered as major storm events. The statistical summary of the satellite measurements with rain gauge observations for the eleven-days for the early, late and final runs are shown in tables 7, 8, and 9, respectively.

The tables indicate that the values of POD and CSI are the same for all events because the precipitation observed by the satellite, but not observed by the gauge does not exist in our analyzed data. Overall, for IMERG early run, the POD and CSI were varied from 0.68 to 1. On the other hand, IMERG late product revealed a major improvement in detecting the precipitation by leveling up the POD as well as the CSI with values ranging from 0.71 to 1. The final run product (table 9) showed a high level of perfection in detecting the precipitation events with very high values of POD and CSI compared to the other IMERG products. In general, the accuracy of detection of the precipitation events by the GPM satellite can be considered perfect due to the high values of POD and the CSI for the three products as shown in tables 7,8 and 9.

In addition, the results depicted that the Correlation Coefficient (CC) for IMERG early run product for all events varies from 0.02 to 0.33, except for the events observed in April 2016. These events have CC varies from 0.5 to 0.75 which were more correlated than the

2015 events. However, for IMERG late run product (table 8) the CC enhanced significantly for the same events with more than (150% on the Avg.). In contrast, IMERG final run (table 9) showed high CC values compared to the other runs, which indicate good correlation between satellite measurements and rain gauge observations when using final data set.

Finally, in terms of errors, the results of ME, RMSE and RB indicate that for all events the errors and bias of the satellite estimates compared with the rain gauge observations were relatively low except for two events which occurred on the 17th of November and the 2nd of December 2015, where high values of ME and RB were observed for both the early and late runs. These parameters decreased significantly in compare with the final run product. The ME for IMERG early run product ranging from -15mm to 32mm, while it reduced on average for IMERG late run and final run products by 40% and >54%, respectively. The RB and the RMSE also exhibited the same trend of the mean error (see tables 5,6,7). Overall the ME, RSME, and RB showed significant improvement between GPM products. The ME, RSME, and RB values decrease from early run to late run and from late run to the final run product which concludes that the error and bias of the satellite estimates in compare with the rain gauge observations are low for the final run product when compared to others.

Table 7: Summary of event-based evaluation for all rain events using the IMERG early run product.

Event Date	Probability of Detection (POD)	Critical Success Index (CSI)	Correlation Coefficient (CC)	Mean Error (ME)	Root Mean Squared Error (RMSE)	Relative Bias (RB)
28-10-2015	0.74	0.74	0.03	-6.32	17.31	-2.19
16-11-2015	0.68	0.68	0.02	6.48	30.88	1.48
17-11-2015	0.9	0.9	0.12	18.72	33.42	6.29
16+17-11	0.87	0.87	0.04	15.18	33.22	2.09
23-11-2015	0.88	0.88	0.24	-0.43	12.79	-0.07
24-11-2015	0.87	0.87	0.22	-10.23	24.31	-0.79
23+24-11	0.91	0.91	0.33	-8.61	24.96	-0.44
2-12-2015	1	1	0.18	32.61	51.44	8.2
23-12-2015	0.73	0.73	0.13	-6.18	10.63	-1.34
30-12-2015	0.89	0.89	0.005	0.89	8.37	0.4
4-04-2016	0.88	0.88	0.75	-8.26	12.81	-1.25
12-04-2016	0.97	0.97	0.24	0.78	16.68	0.1
13-04-2016	0.97	0.97	0.53	-15.06	25.69	-1.58
12+13-04	1	1	0.42	-4.76	21.09	-0.28

Table 8: Summary of event-based evaluation for all rain events using the IMERG late run product.

Event Date	Probability of Detection (POD)	Critical Success Index (CSI)	Correlation Coefficient (CC)	Mean Error (ME)	Root Mean Squared Error (RMSE)	Relative Bias (RB)
28-10-2015	0.85	0.85	0.07	-5.71	17.92	-1.98
16-11-2015	0.71	0.71	0.15	6.7	33.7	1.53
17-11-2015	0.93	0.93	0.2	18.45	29.53	6.2
16+17-11	0.89	0.89	0.002	14.69	31.95	1.99
23-11-2015	0.89	0.89	0.33	2.04	13.62	0.31
24-11-2015	0.94	0.94	0.14	-8.61	25.38	-0.67
23+24-11	0.93	0.93	0.29	-5.2	26.76	-0.27
2-12-2015	1	1	0.27	48.39	64.67	12.16
23-12-2015	0.82	0.82	0.09	-5.34	10.47	-1.16
30-12-2015	0.95	0.95	0.11	1.67	8.6	0.75
4-04-2016	0.98	0.98	0.74	-5.31	12.07	-0.81
12-04-2016	0.97	0.97	0.35	2.63	17.45	0.35
13-04-2016	0.97	0.97	0.51	-4.42	22.34	-0.46
12+13-04	0.99	0.99	0.57	0.45	19.3	0.03

Table 9: Summary of event-based evaluation for all rain events using the IMERG final run product.

Event Date	Probability of Detection (POD)	Critical Success Index (CSI)	Correlation Coefficient (CC)	Mean Error (ME)	Root Mean Squared Error (RMSE)	Relative Bias (RB)
28-10-2015	0.97	0.97	0.008	-4.95	17.14	-1.72
16-11-2015	0.75	0.75	0.085	-6.79	17.63	-1.55
17-11-2015	0.93	0.93	0.282	4.48	14.64	1.51
16+17-11	0.89	0.89	0.127	-0.17	16.07	-0.02
23-11-2015	0.96	0.96	0.31	3.08	14.58	0.47
24-11-2015	0.98	0.98	0.403	-2.77	20.26	-0.22
23+24-11	0.99	0.99	0.435	0.39	24.83	0.02
2-12-2015	1	1	0.287	5.47	12.26	1.38
23-12-2015	0.89	0.89	0.24	-5.73	10.19	-1.24
30-12-2015	0.91	0.91	0.344	-0.48	6.24	-0.22
4-04-2016	0.96	0.96	0.577	-5.11	13.83	-0.78
12-04-2016	0.99	0.99	0.341	4.36	17.99	0.58
13-04-2016	1	1	0.576	-4.34	25.62	-0.45
12+13-04	1	1	0.53	1.81	22.02	0.11

CHAPTER 6

CONCLUSIONS AND RECOMMENDATIONS

Hydrometeorological and climatological applications of satellite precipitation products are witnessing a significant leap with the emergence of the latest satellite product; namely, Integrated Multi-satellitE Retrievals for Global Precipitation Measurement (IMERG) product with spatial and temporal resolutions of 0.1º x 0.1º (approximately 11 Km for latitude and longitude) and 30 minutes, respectively. The IMERG product is based on the Global Precipitation Mission (GPM) to consolidate and enhance precipitation measurements from a constellation of research and operational microwave sensors.

The aim of this research is to evaluate the IMERG satellite rainfall products (early run, late run, and final run product) using ground-based rain gauge observations as a reference all over Saudi Arabia for the period from October 2015 to April 2016. The evaluation was carried out using six commonly statistical measures: Mean Error (ME), Root Mean Squared Error (RMSE), Relative Bias (RB), Correlation Coefficient (CC) Probability of Detection (POD), and Critical Success Index (CSI). Three main comparisons or evaluations have been conducted which are: region-based evaluation, station-based evaluation and event-based evaluation. The main finding of this research are as follows:

The region-based evaluation showed a low errors and bias for Eastern Region, Riyadh, Madinah, and Qassim (Eastern, Middle and southern and part of the western of Saudi Arabia) for IMERG early run, late run and final run products. While for Tabuk, Al-Jouf, Northern Border, and Hail the results indicate a relatively high value of the errors and the bias for the early run and late run products. However, for the final run product, the errors

and the bias reduced significantly leaving only Tabuk and Al-Jouf with relatively high values. In addition, the correlation coefficient (CC) between the satellite measurements and the rain gauge observations based on the early, late and final runs found to be high for Riyadh, Tabuk, Jazan, Al-Jouf and Hail compared with the other regions. Furthermore, the correlation results experienced a remarkable improvement for the final run product such that more than 70% of the total Saudi Arabia's land has a CC value more than 0.5. Moreover, in terms of the accuracy of the satellite detection, all IMERG products tends to have a consistency in detecting the precipitation events. Though, the final run product has a high detection accuracy when compared with an early run and late run products.

The station-based evaluation disclosed high bias and error for the stations located on northern and the north-western parts of Saudi Arabia for IMERG early run product, while the middle and the southern part have moderate values of the estimating errors. Conversely, the eastern part and portion of the western part have a very low bias and estimating error indicating better estimate compared to the other parts of Saudi Arabia. On the other hand, the station-based evaluation revealed a decrease of the bias and the estimating errors for the late run product on the southern part, as well as the western part; however, still the northern and the middle parts of Saudi Arabia, suffer a high estimating errors and bias. On the contrary, the final run product showed a significant improvement over more than 80% of Saudi Arabia's parts. In terms of the correlation between the satellite estimates and ground-based observations, southern, northern and the top eastern parts of Saudi Arabia proven to have a high correlated data for the early run product. The other parts observe a high variation due to the heterogeneity of the hydrological cycle during the rainy season. On the other hand, for the late and final runs the results enhanced significantly in for the

southern and eastern regions. However; in the northern part, the correlation was reduced in the late run due to high bias in the estimation of the precipitation. Nevertheless, the northern part CC measures show some improvement when using the final run product. The other parts of the Kingdom showed a high CC variations due to the heterogeneity of the rainfall distribution and the variation of the topography of the land especially the middle and the western regions of Saudi Arabia. Furthermore, the detection of the satellite to the rain event showed a level of perfection for all IMERG products. In conclusion, even-based evaluation showed that the final run product had the best detection among the other products.

For the event-based evaluation, the IMERG final run product showed a significant accuracy among the other IMERG products. This claim supported by the finding when each event has a high correlation between the satellite and ground observations compared with the IMERG early and late run products. Also, the mean error, relative bias, and root mean squared error proven to be a relatively low for the final run product when setting side by side to the other products. Nevertheless, the results revealed another interesting part when the probability of detection and critical success index parameters are remarkably high for the final run product compared with the other IMERG product. Thus, the overall performance of the IMERG in detecting the precipitation events through the final run product is better than the other products. In addition, the results showed a high error and bias for two events 17th of November and 2nd of December 2015 using the early run and late run product. While for final product the error and the bias for the same events decreased by 50% to the minimum.

In general, the poor results observed with the northern and the southern parts of Saudi Arabia can be attributed to the inherent characteristics of these regions which suffer from

high heterogeneity of the rainfall distribution incorporated with the high variability of the land topography. In addition, many researchers indicate that the satellite accuracy is quite low in detecting the precipitation in the high latitudes, which reveal the poor results of the southern region. Moreover, the northern region has spare rain gage stations compared with the middle and western part. This few number of stations increase the chance to develop more error and bias in the estimation of the precipitation as these stations inadequate to represent the variability of the precipitation distribution pattern.

Overall, the results revealed that the IMERG final run product could have a potential to play a significant role in complementing or substitution for ground precipitation measurements offering reliable products for ungauged or poorly gauged regions. In addition, GPM products are available at high spatial and temporal resolutions, which makes them useful in many hydrological applications in regions like Saudi Arabia that have sparse rain gauge stations. Moreover, the performance measures figures revealed acceptable results for IMERG near-real-time products in most of Saudi Arabia's regions, so these products can be used to conduct hydrological studies such as flood early warning systems or any other applications that required a near-real-time rainfall data.

References

[1] C. Kidd and G. Huffman, "Global precipitation measurement," *Meteorol. Appl.*, vol. 18, no. 3, pp. 334–353, 2011.

[2] E. E. Ebert, J. E. Janowiak, and C. Kidd, "Comparison of near-real-time precipitation estimates from satellite observations and numerical models," *Bull. Am. Meteorol. Soc.*, vol. 88, no. 1, pp. 47–64, 2007.

[3] Z. Li, D. Yang, and Y. Hong, "Multi-scale evaluation of high-resolution multi-sensor blended global precipitation products over the Yangtze River," *J. Hydrol.*, vol. 500, pp. 157–169, 2013.

[4] H. Wu, R. F. Adler, Y. Hong, Y. Tian, and F. Policelli, "Evaluation of Global Flood Detection Using Satellite-Based Rainfall and a Hydrologic Model," *J. Hydrometeorol.*, vol. 13, no. 4, pp. 1268–1284, 2012.

[5] M. Heistermann and D. Kneis, "Benchmarking quantitative precipitation estimation by conceptual rainfall-runoff modeling," *Water Resour. Res.*, vol. 47, no. 6, pp. 1–23, 2011.

[6] S. Sorooshian *et al.*, "Advanced concepts on remote sensing of precipitation at multiple scales," *Bull. Am. Meteorol. Soc.*, vol. 92, no. 10, pp. 1353–1357, 2011.

[7] C. Kidd, V. Levizzani, J. Turk, and R. Ferraro, "Satellite precipitation measurements for water resource monitoring," *J. Am. Water Resour. Assoc.*, vol. 45, no. 3, pp. 567–579, 2009.

[8] J. Thornes *et al.*, "Communicating the value of atmospheric services," *Meteorol. Appl.*, vol. 17, no. 2, pp. 243–250, 2010.

[9] S. Michaelides, V. Levizzani, E. Anagnostou, P. Bauer, T. Kasparis, and J. E. Lane, "Precipitation: Measurement, remote sensing, climatology and modeling," *Atmos. Res.*, vol. 94, no. 4, pp. 512–533, 2009.

[10] S. Hag-elsafi and M. El-tayib, "Spatial and statistical analysis of rainfall in the Kingdom of Saudi Arabia from 1979 to 2008," *Weather*, pp. 262–266, 2016.

[11] M. Al-Zahrani and T. Husain, "An algorithm for designing a precipitation network in the south-western region of Saudi Arabia," *J. Hydrol.*, vol. 205, no. 3–4, pp. 205–216, 1998.

[12] Z. Şen and K. Al-Suba'I, "Hydrological considerations for dam siting in arid regions: a Saudi Arabian study," *Hydrol. Sci. J.*, vol. 47, no. 2, pp. 173–186, 2002.

[13] M. A. Abdullah and M. A. Al-Mazroui, "Climatological study of the southwestern

region of Saudi Arabia. I. Rainfall analysis," *Clim. Res.*, vol. 9, no. 3, pp. 213–223, 1998.

[14] H. Hasanean and M. Almazroui, "Rainfall: Features and Variations over Saudi Arabia, A Review," *Climate*, vol. 3, no. 3, pp. 578–626, 2015.

[15] M. Almazroui, "Calibration of TRMM rainfall climatology over Saudi Arabia," *Atmos. Res.*, vol. 99, no. 3–4, pp. 400–414, 2011.

[16] The Ministry of Hydrology, "Water Atlas of Saudi Arabia," Riyadh, Saudi Arabia, 1984.

[17] M. Al-Mazroui, "Climatological study over the southwestern region of the Kingdom of Saudi Arabia with special reference to rainfall distribution," King Abdulaziz University, Jeddah, Saudi Arabia, 1998.

[18] a M. Subyani, "Geostatistical study of annual and seasonal mean rainfall patterns in southwest Saudi Arabia," *Hydrol. Sci. Journal-Journal Des Sci. Hydrol.*, vol. 49, no. October 2004, pp. 803–817, 2004.

[19] Y. Tian, C. D. Peters-Lidard, B. J. Choudhury, and M. Garcia, "Multitemporal Analysis of TRMM-Based Satellite Precipitation Products for Land Data Assimilation Applications," *J. Hydrometeorol.*, vol. 8, pp. 1165–1183, 2007.

[20] S. G. Dixon and R. L. Wilby, "Forecasting reservoir inflows using remotely sensed precipitation estimates: a pilot study for the River Naryn, Kyrgyzstan," *Hydrol. Sci. J.*, vol. 6667, no. January, p. 150113093103002, 2015.

[21] G. Tang, Y. Ma, D. Long, L. Zhong, and Y. Hong, "Evaluation of GPM Day-1 IMERG and TMPA Version-7 legacy products over Mainland China at multiple spatiotemporal scales," *J. Hydrol.*, vol. 533, pp. 152–167, 2016.

[22] H. Guo *et al.*, "Early assessment of Integrated Multi-satellite Retrievals for Global Precipitation Measurement over China," *Atmos. Res.*, vol. 176–177, pp. 121–133, 2016.

[23] S. Ning, J. Wang, J. Jin, and H. Ishidaira, "Assessment of the Three Latest GPM-era High Resolution Satellite Precipitation Products against Gauged Data over the Chinese Mainland : Initial Results," pp. 1–16, 2016.

[24] M. Li and Q. Shao, "An improved statistical approach to merge satellite rainfall estimates and raingauge data," *J. Hydrol.*, vol. 385, no. 1–4, pp. 51–64, 2010.

[25] F. J. Tapiador *et al.*, "Global precipitation measurement: Methods, datasets and applications," *Atmos. Res.*, vol. 104–105, pp. 70–97, 2012.

[26] Z. Ren and M. Li, "Errors and correction of precipitation measurements in China,"

Adv. Atmos. Sci., vol. 24, no. 3, pp. 449–458, 2007.

[27] G. J. Ciach, "Local random errors in tipping-bucket rain gauge measurements," *J. Atmos. Ocean. Technol.*, vol. 20, no. 5, pp. 752–759, 2003.

[28] E. Habib, W. F. Krajewski, and A. Kruger, "Sampling Errors of Tipping-Bucket Rain Gauge Measurements," *J. Hydrol. Eng.*, vol. 6, no. 2, pp. 159–166, 2001.

[29] J. A. Nystuen, "Relative performance of automatic rain gauges under different rainfall conditions," *J. Atmos. Ocean. Technol.*, vol. 16, no. 8, pp. 1025–1043, 1999.

[30] H. M. Ragunath, *Hydrology, Principles, Analysis, Design*. New Age International, 2006.

[31] J. Lane *et al.*, "High spatial resolution rainfall mapping from NASA â€™ s dense rain gauge network," in *In ASAE Florida Section Annual Conference*, 1998.

[32] Fondriest Environmental, "Advanced laser-based disdrometer," 2016. [Online]. Available: http://www.fondriest.com/ott-parsivel2-laser-precipitation-sensor.htm.

[33] U. Germann, G. Galli, M. Boscacci, and M. Bolliger, "Radar precipitation measurement in a mountainous region," *Q. J. R. Meteorol. Soc.*, vol. 132, no. 618, pp. 1669–1692, 2006.

[34] NOAA, "Weather Radar - NOAA," 2005. [Online]. Available: https://commons.wikimedia.org/wiki/File:Doppler_Weather_Radar_-_NOAA.jpg. [Accessed: 30-Oct-2016].

[35] S. Prakash, A. K. Mitra, A. Aghakouchak, Z. Liu, H. Norouzi, and D. S. Pai, "A preliminary assessment of GPM-based multi-satellite precipitation estimates over a monsoon dominated region," *J. Hydrol.*, no. February 2014, pp. 1–12, 2016.

[36] T. Zhou, R. Yu, H. Chen, A. Dai, and Y. Pan, "Summer precipitation frequency, intensity, and diurnal cycle over China: A comparison of satellite data with rain gauge observations," *J. Clim.*, vol. 21, no. 16, pp. 3997–4010, 2008.

[37] S. Sorooshian, K. L. Hsu, X. Gao, H. V. Gupta, B. Imam, and D. Braithwaite, "Evaluation of PERSIANN system satellite-based estimates of tropical rainfall," *Bull. Am. Meteorol. Soc.*, vol. 81, no. 9, pp. 2035–2046, 2000.

[38] R. J. Joyce, J. E. Janowiak, P. a. Arkin, and P. Xie, "CMORPH: A Method that Produces Global Precipitation Estimates from Passive Microwave and Infrared Data at High Spatial and Temporal Resolution," *J. Hydrometeorol.*, vol. 5, no. 3, pp. 487–503, 2004.

[39] Y. Hong, K.-L. Hsu, S. Sorooshian, and X. Gao, "Precipitation Estimation from Remotely Sensed Imagery Using an Artificial Neural Network Cloud Classification

System," *J. Appl. Meteorol.*, vol. 43, pp. 1834–1853, 2004.

[40] G. J. Huffman *et al.*, "The TRMM Multisatellite Precipitation Analysis (TMPA): Quasi-Global, Multiyear, Combined-Sensor Precipitation Estimates at Fine Scales," *J. Hydrometeorol.*, vol. 8, no. 1, pp. 38–55, 2007.

[41] T. Kubota *et al.*, "Global precipitation map using satelliteborne microwave radiometers by the GSMaP project: Production and validation," *Int. Geosci. Remote Sens. Symp.*, vol. 45, no. 7, pp. 2584–2587, 2006.

[42] R. A. Scofield and R. J. Kuligowski, "Status and Outlook of Operational Satellite Precipitation Algorithms for Extreme-Precipitation Events," *Weather Forecast.*, vol. 18, no. 6, pp. 1037–1051, 2003.

[43] G. A. Vicente, R. A. Scofield, and W. P. Menzel, "The 0perational GOES infrared rainfall estimation technique," *Bull. Am. Meteorol. Soc.*, vol. 79, no. 9, pp. 1883–1898, 1998.

[44] R. F. Adler and A. J. Negri, "A Satellite Infrared Technique to Estimate Tropical Convective and Stratiform Rainfall," *J. Appl. Meteorol.*, vol. 27, no. 1, pp. 30–51, 1988.

[45] P. Arkin and B. Meisner, "The relationship between large-scale convective rainfall and cold cloud over the western hemisphere during 1982-84," *Mon. Weather Rev.*, vol. 115, pp. 51–74, 1987.

[46] K. P. Bowman, "Comparison of TRMM precipitation retrievals with rain gauge data from ocean buoys," *J. Clim.*, vol. 18, no. 1, pp. 178–190, 2005.

[47] A. K. Shukla, C. S. P. Ojha, and R. D. Garg, "Satellite based estimation and validation of monthly rainfall distribution over upper ganga river basin," *Int. Arch. Photogramm. Remote Sens. Spat. Inf. Sci. - ISPRS Arch.*, vol. XL-8, no. 1, pp. 399–404, 2014.

[48] X. Li, Q. Zhang, and C. Y. Xu, "Assessing the performance of satellite-based precipitation products and its dependence on topography over Poyang Lake basin," *Theor. Appl. Climatol.*, vol. 115, no. 3–4, pp. 713–729, 2014.

[49] E. Sharifi, R. Steinacker, and B. Saghafian, "Assessment of GPM-IMERG and Other Precipitation Products against Gauge Data under Different Topographic and Climatic Conditions in Iran: Preliminary Results," *Remote Sens.*, vol. 8, no. 2, p. 135, 2016.

[50] NASA, "Constellation Partners | Precipitation Measurement Missions," 2011. [Online]. Available: http://pmm.nasa.gov/GPM/constellation-partners. [Accessed: 20-Feb-2016].

[51] NASA, “Global Precipitation Measurement (GPM) Mission Overview | Precipitation Measurement Missions,” 2011. [Online]. Available: http://pmm.nasa.gov/GPM. [Accessed: 20-Feb-2016].

[52] G. J. Huffman *et al.*, “NASA Global Precipitation Measurement (GPM) Integrated Multi-satellitE Retrievals for GPM (IMERG),” no. November, p. 26, 2015.

[53] NASA, “GPM Data Downloads | Precipitation Measurement Missions,” 2014. [Online]. Available: http://pmm.nasa.gov/data-access/downloads/gpm. [Accessed: 20-Feb-2016].

[54] Ministry of Water and Electricity (MOWE), “Rain gauge summary over the Kingdom of Saudi-Arabia,” 2016. [Online]. Available: http://app.mowe.gov.sa/DailyRainsNews/Rain_Dams.aspx.

[55] M. Kheimi and R. Sultana, “Assessment of Remotely-Sensed precipitation products across the Saudi Arabia Region,” *AGU Fall Meet. Abstr.*, vol. 1, p. 448, 2012.

[56] WeatherOnline LTD, “Climate of the World: Iceland - Weather UK - weatheronline.co.uk,” 2015. [Online]. Available: http://www.weatheronline.co.uk/reports/climate/Iceland.htm. [Accessed: 19-Feb-2016].

[57] B. Yong *et al.*, “Hydrologic evaluation of Multisatellite Precipitation Analysis standard precipitation products in basins beyond its inclined latitude band: A case study in Laohahe basin, China,” *Water Resour. Res.*, vol. 46, no. 7, pp. 1–20, 2010.

Appendix-A

List of Ministry of Water and Electricity (MOWE) rain-gauge stations

This appendix contains the list of the Ministry of Water and Electricity (MOWE) stations distributed all over Saudi Arabia used in this study.

No	Region	Station ID	Station Name (English)	Easting	Northing	Altitude	Zone
1	Riyadh	RD1	Alkharaj	741819	2680615	468	38
2		RD2	Ushaiger	518449	2802886	710	38
3		RD3	Alajabilh	648171	2750982	615	38
4		RD4	Alhariq	654728	2612608	540	38
5		RD5	Al-Dalam	720245	2655581	449	38
6		RD6	Al-Dawadimi	444043	2714649	971	38
7		RD7	Al-Zulfi	480033	2907077	670	38
8		RD8	Al-Sabila	667907	2741577	649	38
9		RD9	Ghat	496081	2878638	669	38
10		RD10	Almujmaea	535062	2862811	688	38
11		RD11	Almuzahimia	627287	2708195	622	38
12		RD12	Factories Station in Riyadh	673848	2718050	564	38
13		RD13	Thadeq	562059	2802001	670	38
14		RD14	harimla'	629280	2789556	645	38
15		RD15	hutat bani tamim	687206	2600066	525	38
16		RD16	Hawtat Sadir	684102	2833430	730	38
17		RD17	Suwaidi District	669090	2720576	626	38
18		RD18	Jerusalem neighborhood	677382	2738803	625	38
19		RD19	Alnnamudhajia neighborhood	671390	2727958	599	38
20		RD20	Ramah	715982	2829446	520	38
21		RD21	Sdos	520185	2763117	626	38
22		RD22	Shuqara'	525176	2792654	730	38
23		RD23	Durama'	613034	2722962	630	38
24		RD24	Eafyf	289658	2648385	940	38
25		RD25	Ealaqa	478657	2913448	615	38
26		RD26	Marrat	511762	2777871	516	38
27		RD27	Khurub Farms	519209	2798734	718	38
28		RD28	The ministry warehouse at AlMalaz	681689	2733935	609	38
29		RD29	Wadi Hanifa	663589	2729002	625	38
30		RD30	Ministry of Water and Electricity	667768	2736852	644	38
31		RD31	Wadi Aldawasir	479141	2263136	750	38
32		RD32	Thadig Dam	562059	2802001	670	38
33		RD33	Suwaidi District / Automatic	669090	2720576	626	38
34		RD34	Algowayeeya	523717	2663472	853	38
35		RD35	Al Aziziyah / Automatic	733426	2672564	432	38
36		RD36	Al-Zulfi / Automatic	480032	2907077	670	38
37		RD37	Alhariq / Automatic	654727	2612607	540	38

38		RD38	Alajabilh / Automatic	648170	2750981	615	38
39	**Makkah**	MK1	Wadi Huly	772346	2076986	90	37
40		MK2	Makkah	584630	2370327	280	37
41		MK3	kalakh	686697	2358261	1390	37
42		MK4	Ghumyqh	651384	2247189	84	37
43		MK5	Rabgh	503421	2523225	8	37
44		MK6	Dhahban/ Alqunfadhih	719134	2116887	17	37
45		MK7	Khulais	534371	2449468	60	37
46		MK8	South of Jeddah	525037	2355400	25	37
47		MK9	Jeddah Directorate	520716	2377499	11	37
48		MK10	Alqadira	646981	2352320	1670	37
49		MK11	Shifa	641983	2330135	2133	37
50		MK12	Alshshueba	565103	2497534	317	37
51		MK13	Alddar albayda'	681907	2718306	561	38
52		MK14	Bahra	572539	2370268	116	37
53	**Madinah**	MD1	Abyar almashi	523699	2674544	660	37
54		MD2	Om-Dhian	491526	2657920	310	37
55		MD3	Albawir	506730	2759413	681	37
56		MD4	Alhinakih	653264	2747345	849	37
57		MD5	Al-Suiirqiuh	653264	2747345	870	37
58		MD6	Suwaiq	444038	2695672	148	37
59		MD7	Aleaqiluh	560522	2770618	800	37
60		MD8	Alealla	385514	2944493	681	37
61		MD9	Aleis	410837	2771867	644	37
62		MD10	Alfarish	527074	2680086	785	37
63		MD11	Alfaqir	571516	2589819	682	37
64		MD12	Madina El Monawara	559093	2711555	590	37
65		MD13	Almusayjid	508470	2663455	471	37
66		MD14	Almulbina	552884	2562063	389	37
67		MD15	Almahd	689895	2600500	1038	37
68		MD16	Badr	476218	2624722	119	37
69		MD17	Bawat	521391	2735083	503	37
70		MD18	Khaybar	553502	2844415	710	37
71		MD19	Aldilaah	418016	2835331	650	37
72		MD20	Alsoaidara	616349	2733479	870	37
73		MD21	Asalsalah	532729	2792670	850	37
74	**Qassim**	QS1	Alasyah	420486	2964534	543	38
75		QS2	Albadaye	373208	2874206	676	38
76		QS3	Bakeereya	365739	2894266	655	38
77		QS4	Qassim Airport	377604	2909795	650	38
78		QS5	Experiment Station	381198	2862869	724	38

79		QS6	Qabah	407004	2989660	575	38
80		QS7	Euyun Aljawwa'	363691	2931629	648	38
81		QS8	Dariyah	289289	2737023	810	38
82		QS9	Unaiyza	398308	2883463	724	38
83		QS10	Euqlat Alssuqur	217646	2860252	740	38
84		QS11	Shari	351497	3015015	682	38
85		QS12	Riad Alkhubara'	354081	2882406	660	38
86		QS13	Dkhnh	360797	2804423	800	38
87		QS14	Buraidah - Automatic	396876	2913011	602	38
88		QS15	Buraidah	396876	2913011	630	38
89		QS16	Al-Nabhaniyah	306248	2860498	760	38
90		QS17	Almudhannab	411546	2868599	611	38
91		QS18	alfawarih	266254	2884207	818	38
92		QS19	Alshshamasih	425878	2911212	609	38
93		QS20	Alrrss	351373	2861757	725	38
94		QS21	Uyun AlJiwa	363691	2931629	655	38
95	**Eastern Region**	ER1	Om euqlana	NA	NA	NA	
96		ER2	Hofuf airport	347613	2797427	178	39
97		ER3	Research Center at Al-Ahsa	355864	2816440	147	39
98		ER4	Aleulya village	766089	3050774	176	39
99		ER5	Auryerah	286380	2871887	200	39
100		ER6	Salwa	486518	2737272	5	39
101		ER7	Ras Al Khafji	255102	3145903	0	39
102		ER8	Hafr Al-Batin	594364	3145676	317	38
103		ER9	Baqiq	363161	2870860	90	39
104		ER10	Hofuf	355944	2821089	160	39
105		ER11	Qatif	400346	2931445	4.7	39
106		ER12	Assarar	240295	2987281	75	39
107		ER13	Alssadawaa	671920	3109516	320	38
108		ER14	Raqa'i	654286	3207218	306	38
109		ER15	Dammam	420129	2907308	12	39
110		ER16	Al-Ahsa	359411	2832130	150	39
111	**Asir**	AS1	Sabbat Aleilaya	804340	2162418	2284	37
112		AS2	Abalh Blhamr	209930	2068020	2604	38
113		AS3	Bani Thur	255588	2061836	1842	38
114		AS4	Dhahran South	342721	1953771	2149	38
115		AS5	Khatt	187863	2114322	680	38
116		AS6	bilillasamar	210101	2079095	2530	38
117		AS7	Teehan	216390	2029154	2469	38
118		AS8	Sobh Blhamr	211576	2060610	2500	38
119		AS9	Wadis Al Amer	265422	2002659	2222	38

120		AS10	Sarat Eibidih	299020	2009664	2280	38
121		AS11	Tarqash	185085	2066018	400	38
122		AS12	Almajariduh	798095	2116151	450	37
123		AS13	Aleaqiqat Bialnnamas	776839	2241363	1569	37
124		AS14	Alshshaebayn / Rijal almae	203909	2020111	700	38
125		AS15	Alssuduh	221544	2019849	2180	38
126		AS16	Alkhush	803853	2103982	365	37
127		AS17	Alhrijuh	327007	1983569	2283	38
128		AS18	Alhabil / rijal almae	206978	2003342	442	38
129		AS19	Abha	233811	2014139	2170	38
130		AS20	Mahayel	186786	2051772	450	38
131		AS21	Tarybe	311763	2050124	1850	38
132		AS22	Tanumah	201488	2090308	2306	38
133		AS23	Bisha	248917	2215126	1155	38
134		AS24	Alnnamas	197256	2119889	2377	38
135		AS25	Almahalih	242876	2032474	2099	38
136		AS26	Almaoan	243224	2058309	2017	38
137		AS27	Al-tajir	239578	2049130	2065	38
138	**Tabuk**	TK1	Khraibeh	261880	3141729	780	37
139		TK2	Alkr	284341	2949500	277	37
140	**Hail**	HL1	Alhayit	645149	2874027	1067	37
141		HL2	Hail Airport	765519	3037793	1015	37
142		HL3	Alhalifuh Aleulya	678489	2876901	880	37
143		HL4	Sumayra'	212560	2932438	950	38
144		HL5	Mashar Park	759491	3055976	1085	37
145		HL6	Salam neighborhood	763879	3050141	1006	37
146		HL7	Hail	766662	3048414	990	37
147		HL8	Jabbah	690081	3100555	920	37
148		HL9	Baqa'aa'	242355	3085183	755	38
149		HL10	Alghzalh	733640	2964597	980	37
150		HL11	Aleazim	247685	2942784	940	38
151		HL12	Alssalimi	734655	2909193	950	37
152	**Northern Border**	NB1	Arar	692575	3429499	543	37
153		NB2	Tarif	341491	3471439	549	37
154		NB3	lynh	377972	3182775	505	38
155		NB4	Shuebat Nisab	473553	3196228	409	38
156		NB5	Rafha	354933	3279679	448	38
157		NB6	Hazzm Aljalamid	607396	3350709	800	37
158		NB7	Hazzm Aljalamid / Automatic	607396	3350709	800	37
159	**Jazan**	JZ1	Abu-Arish	269286	1877140	69	38
160		JZ2	Alrith	266557	1949132	600	38

161		JZ3	Alearida	299555	1886052	223	38
162		JZ4	Bisha	237888	1921803	70	38
163		JZ5	Jazan	237256	1871982	4	38
164		JZ6	Samtah	281294	1836424	40	38
165		JZ7	Sabya	250274	1898396	71	38
166		JZ8	Sanbah	237256	1871982	0	38
167		JZ9	Dammad	264148	1893804	70	38
168		JZ10	Ayban	290982	1915654	305	38
169		JZ11	Viva	301559	1910015	860	38
170		JZ12	Hurub	281294	1836424	40	38
171		JZ13	Gwz Aljaeafrih	228687	1896084	5	38
172	**Al Baha**	BH1	Almakhawah	754971	2187492	330	37
173		BH2	Alajaadh	770471	2202491	2045	37
174		BH3	Baha	758114	2211536	2259	37
175		BH4	Gari	756343	2213356	2155	37
176		BH5	Almundaq	739371	2233605	1936	37
177		BH6	Galwah	738972	2207573	400	37
178		BH7	Baljurashi	769211	2199210	2051	37
179		BH8	Aleaqiq	776839	2241363	1569	37
180	**Al Jouf**	JF1	Alshshaqiq	588567	3241568	673	37
181		JF2	Issawiya	377119	3398905	559	37
182		JF3	Alnbbuk Abuqusr	466345	3352080	600	37
183		JF4	Dumat Al-Jundal	583756	3296938	650	37
184		JF5	Sakaka	615780	3315697	574	37
185		JF6	Tabarjal	424829	3374452	543	37
186		JF7	Taleat Ammar	649557	3392946	695	37
187		JF8	Eayn Alhiwas	366904	3471839	517	37
188		JF9	Saqat	NA	NA	NA	37
189		JF10	Almarir / Automatic	588368	3324679	700	37

Appendix – B

Spatial distribution of the IMERG precipitation products of the rainfall events

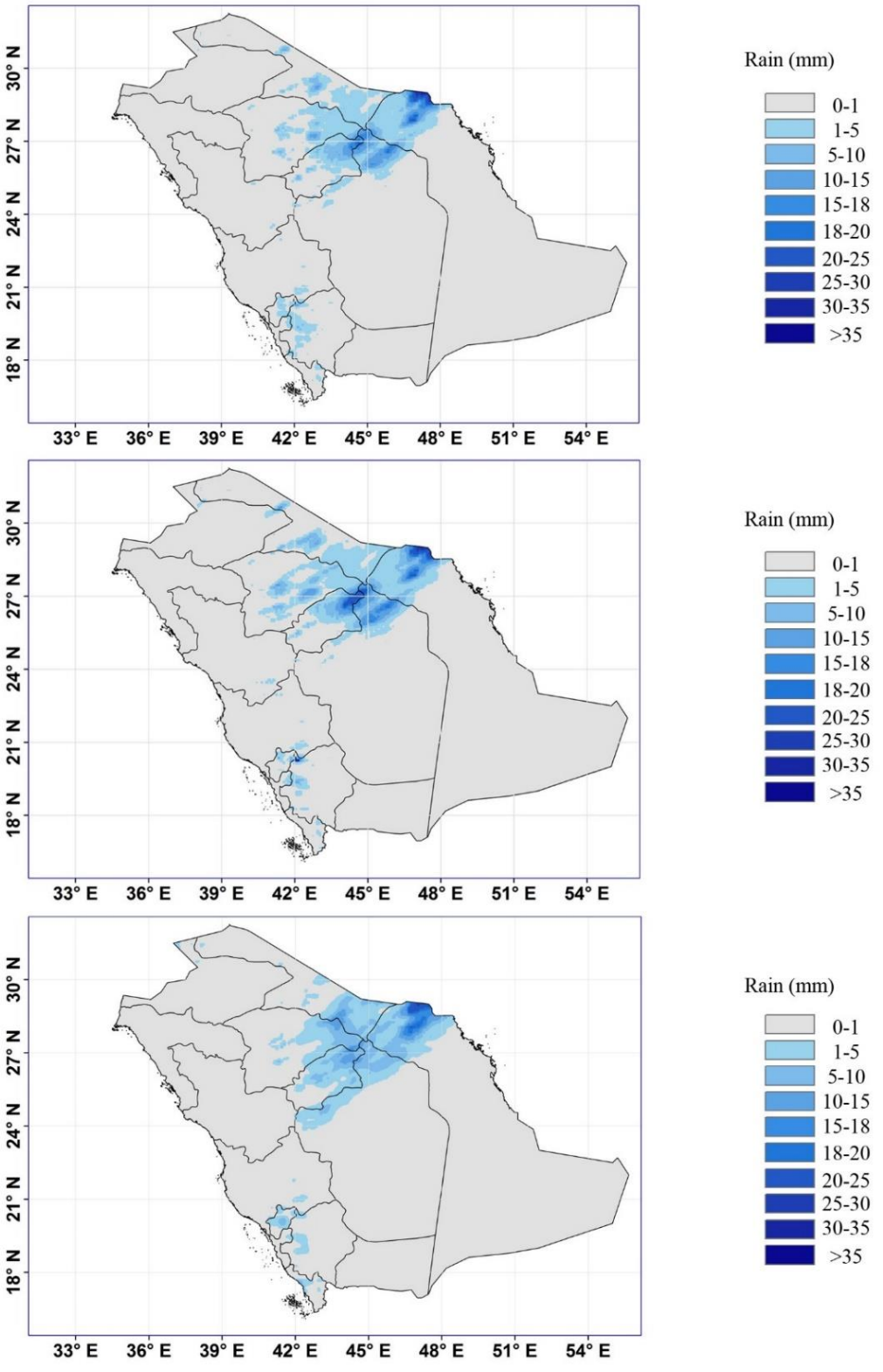

Figure B-1: The spatial distribution of the IMERG Early, Late, and Final run precipitation products. (Date 28-10-2015)

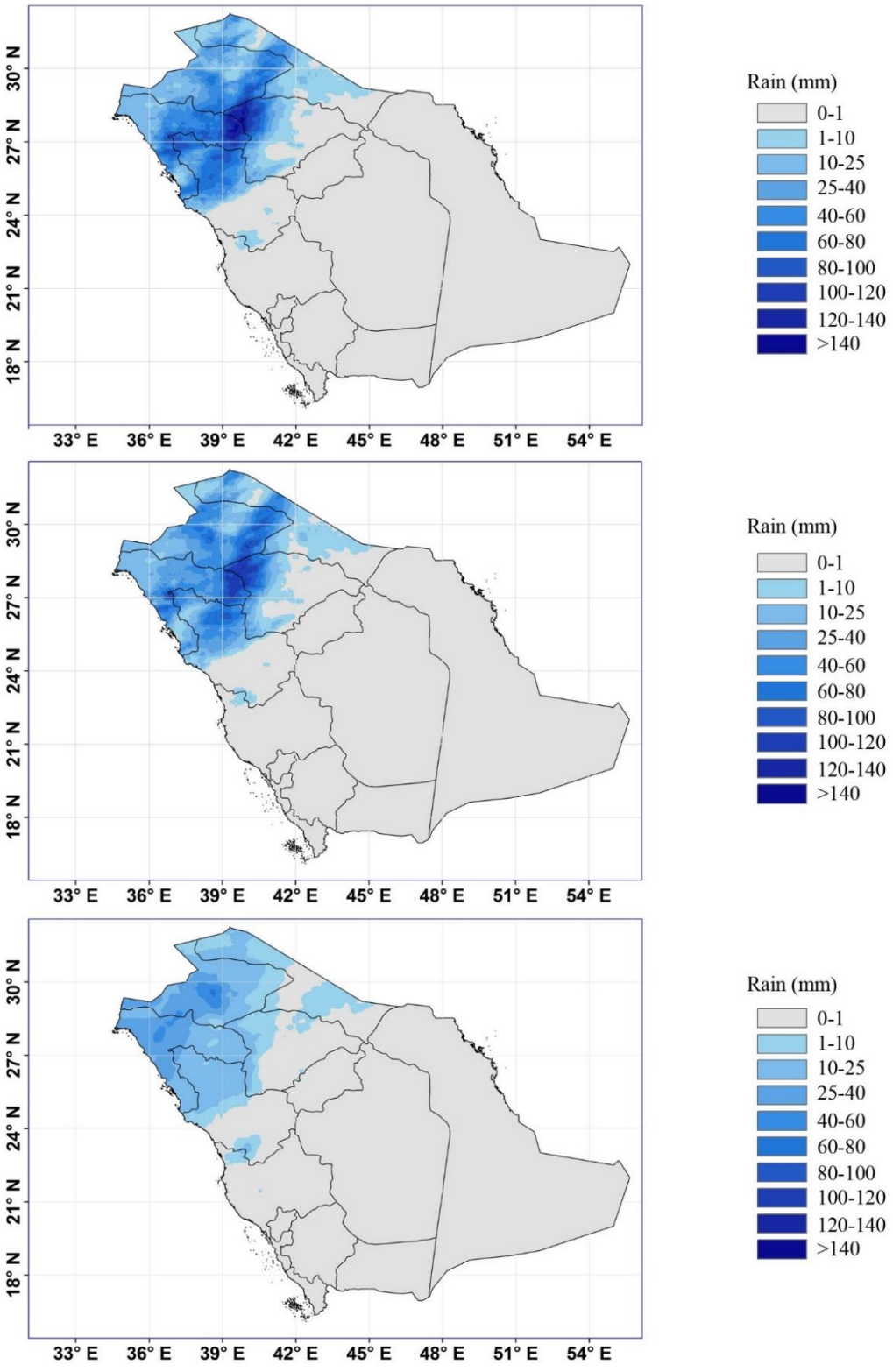

Figure B-2: The spatial distribution of the IMERG Early, Late and Final run precipitation products. (Date 16-11-2015)

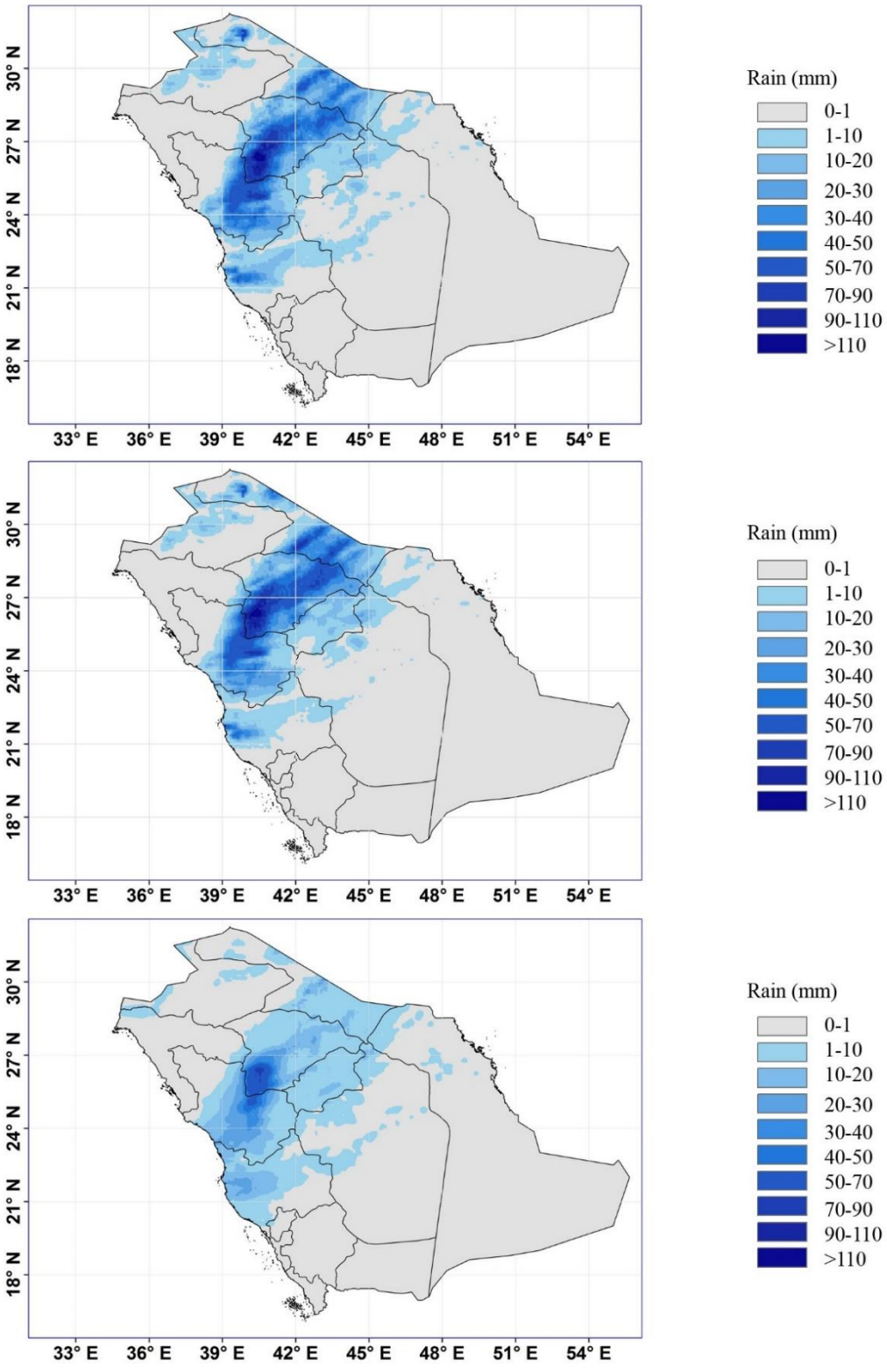

Figure B-3: The spatial distribution of the IMERG Early, Late and Final run precipitation products. (Date 17-11-2015)

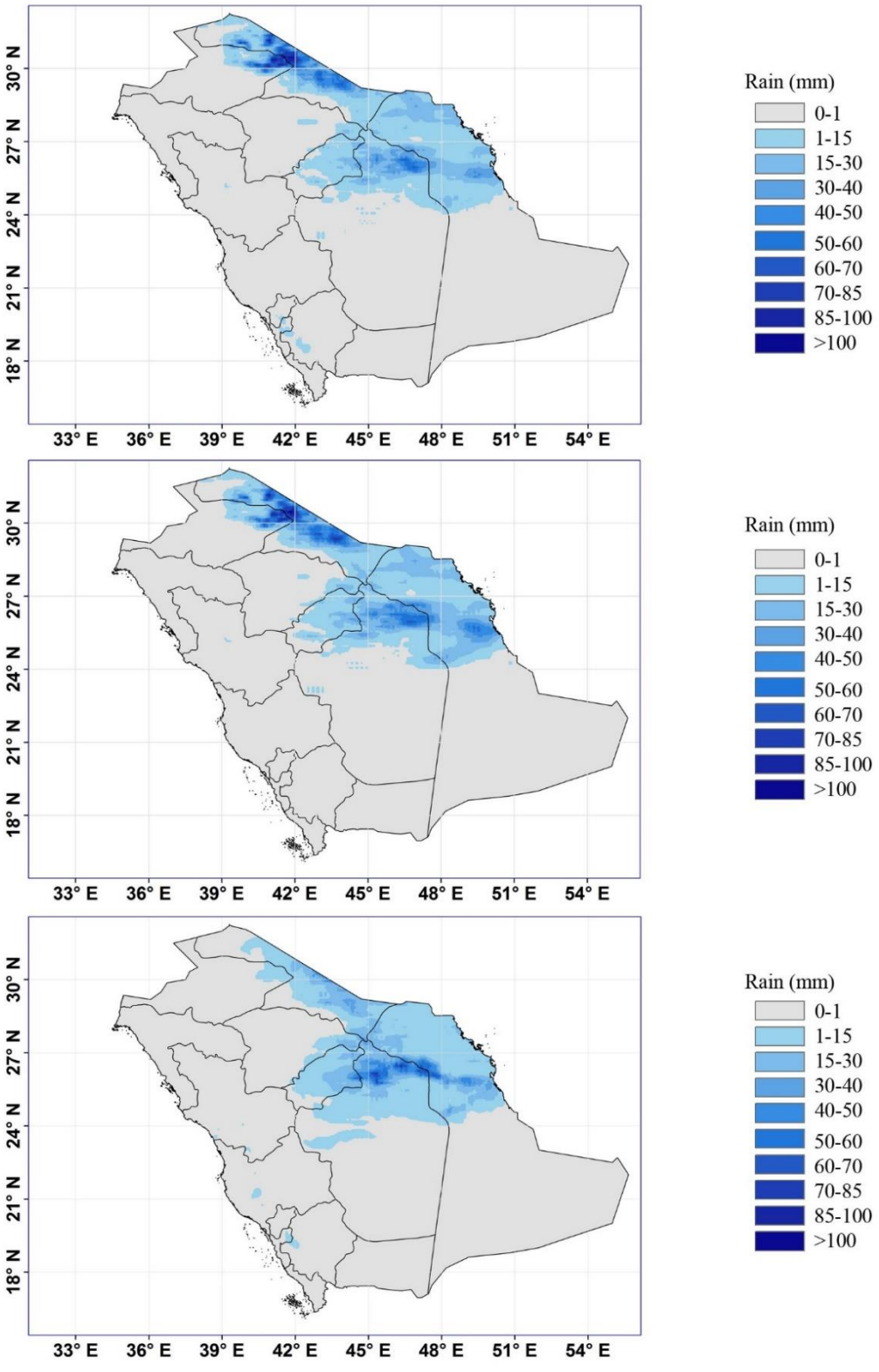

Figure B-4: The spatial distribution of the IMERG Early, Late, and Final run precipitation products. (Date 23-11-2015)

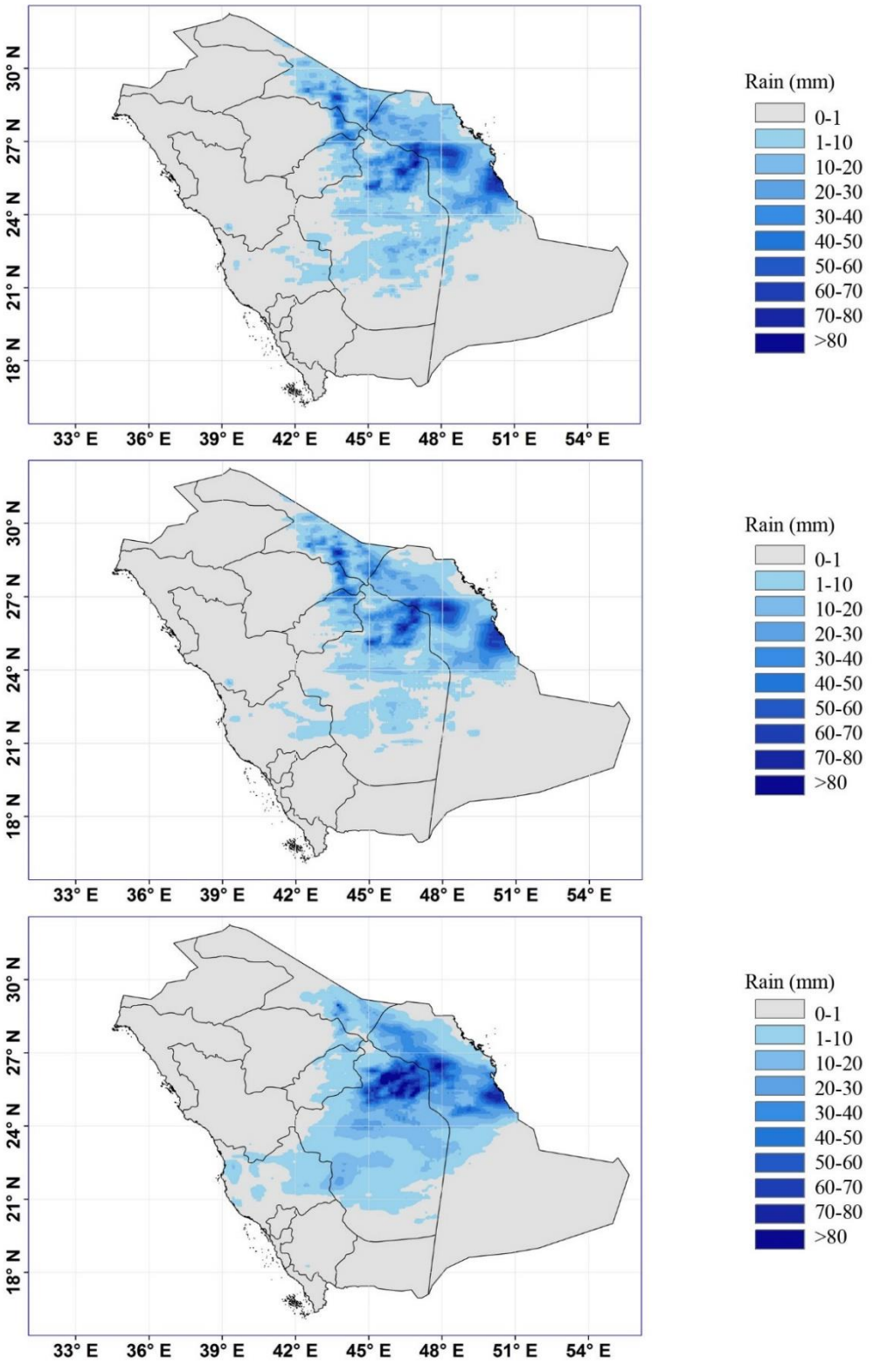

Figure B-5: The spatial distribution of the IMERG Early, Late, and Final run precipitation products. (Date 24-11-2015)

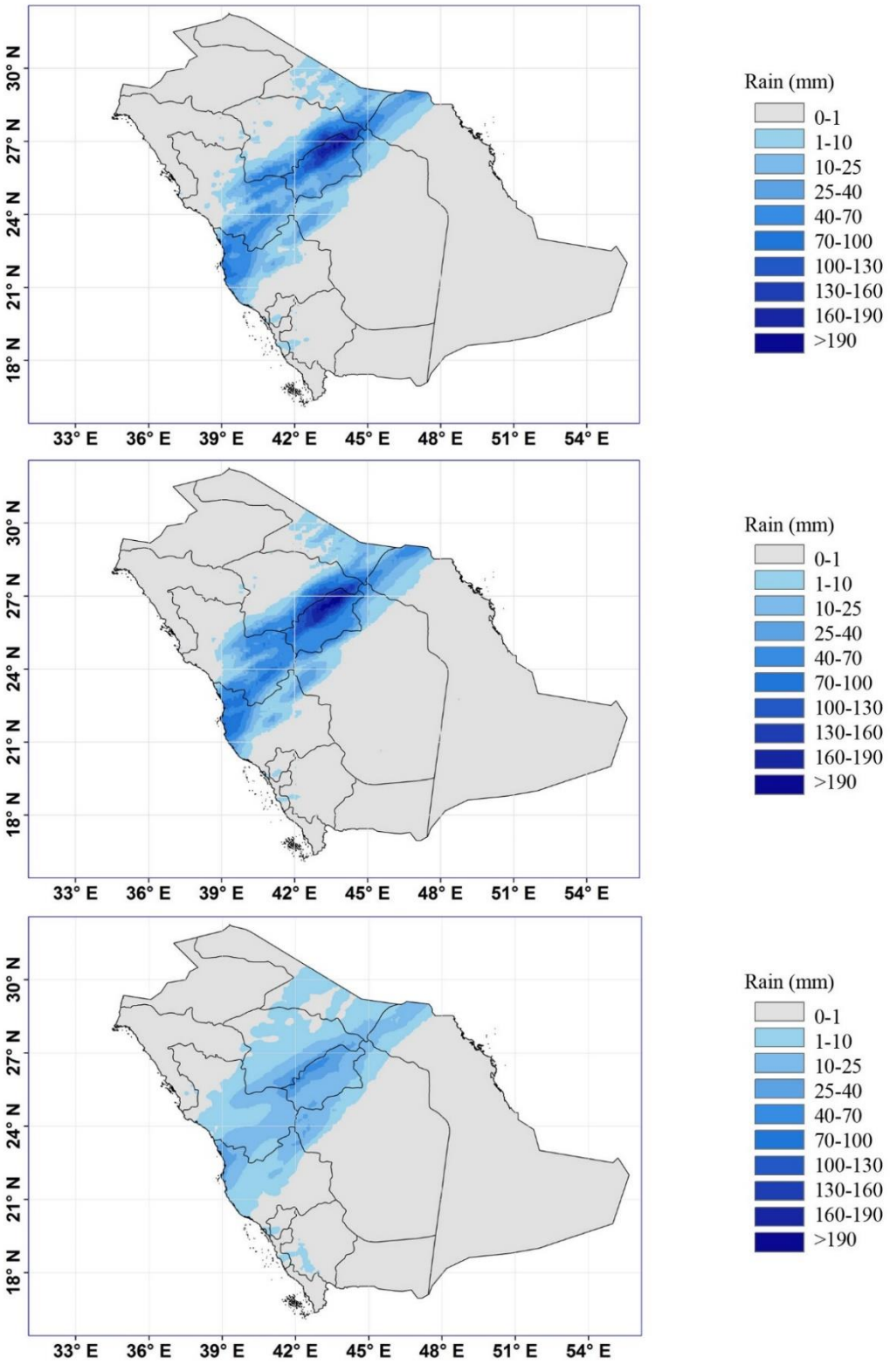

Figure B-6: The spatial distribution of the IMERG Early, Late, and Final run precipitation products. (Date 2-12-2015)

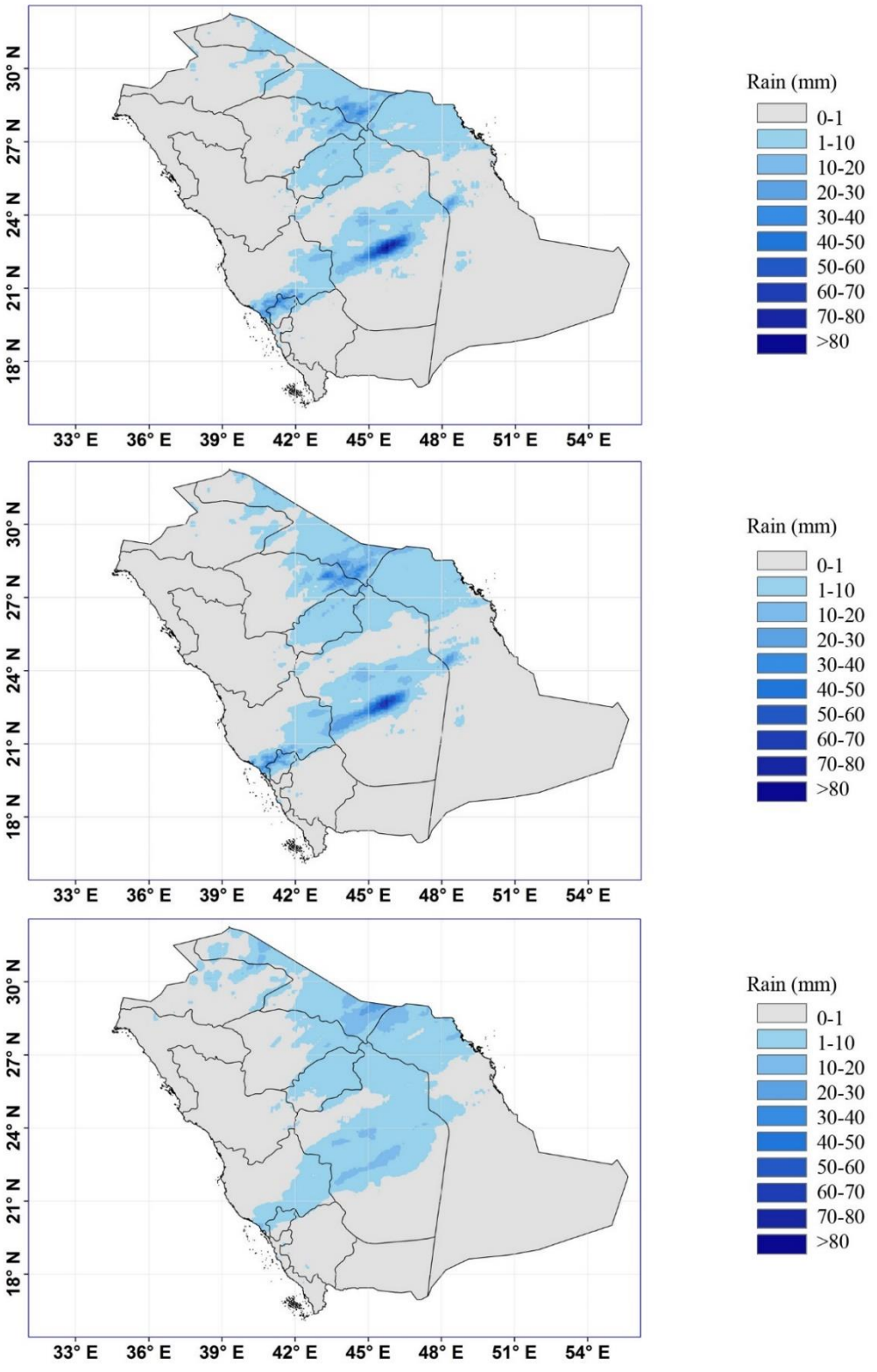

Figure B-7: The spatial distribution of the IMERG Early, Late, and Final run precipitation products. (Date 23-12-2015)

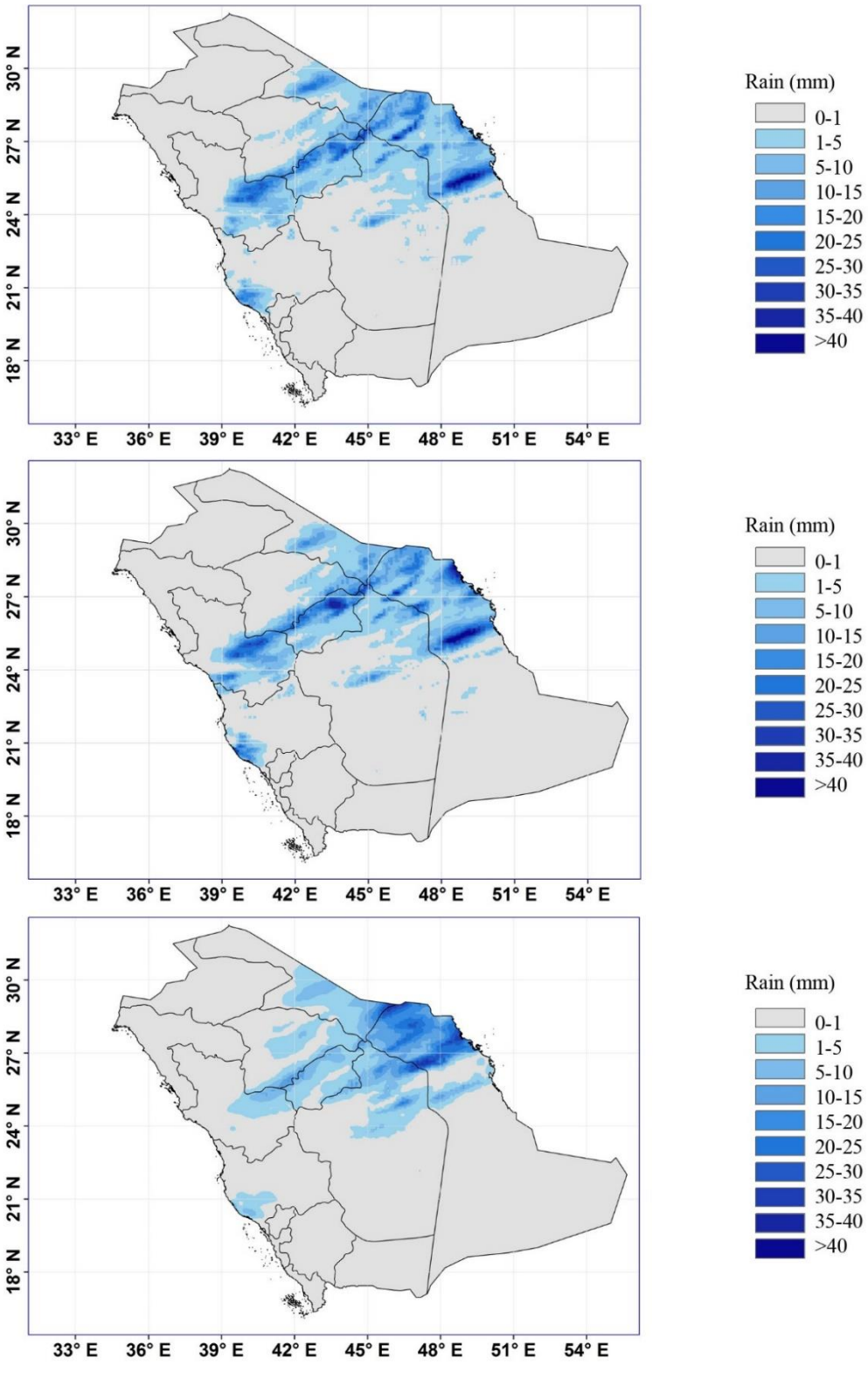

Figure B-8: The spatial distribution of the IMERG Early, Late, and Final run precipitation products. (Date 30-12-2015)

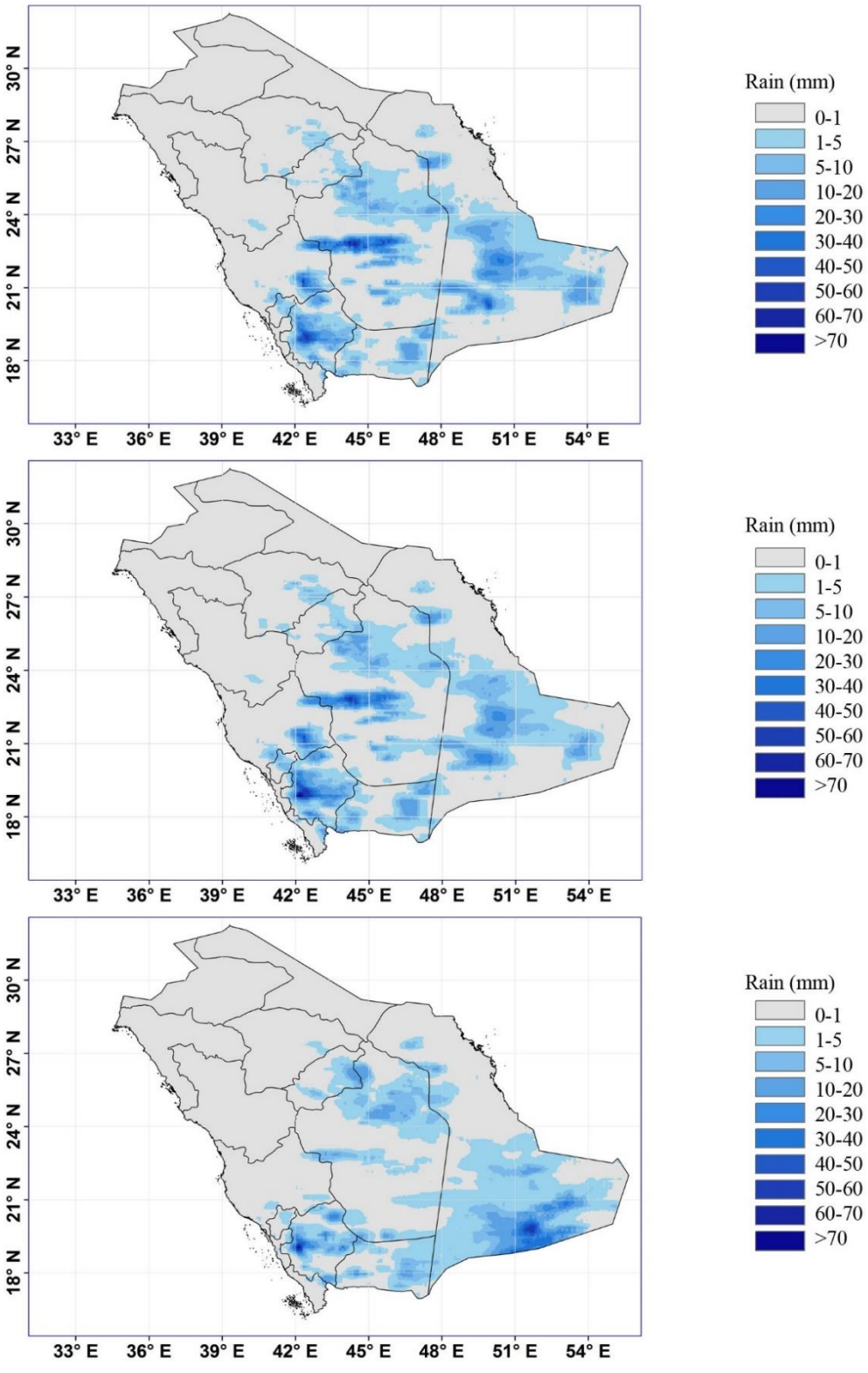

Figure B-9: The spatial distribution of the IMERG Early, Late, and Final run precipitation products. (Date 4-04-2016)

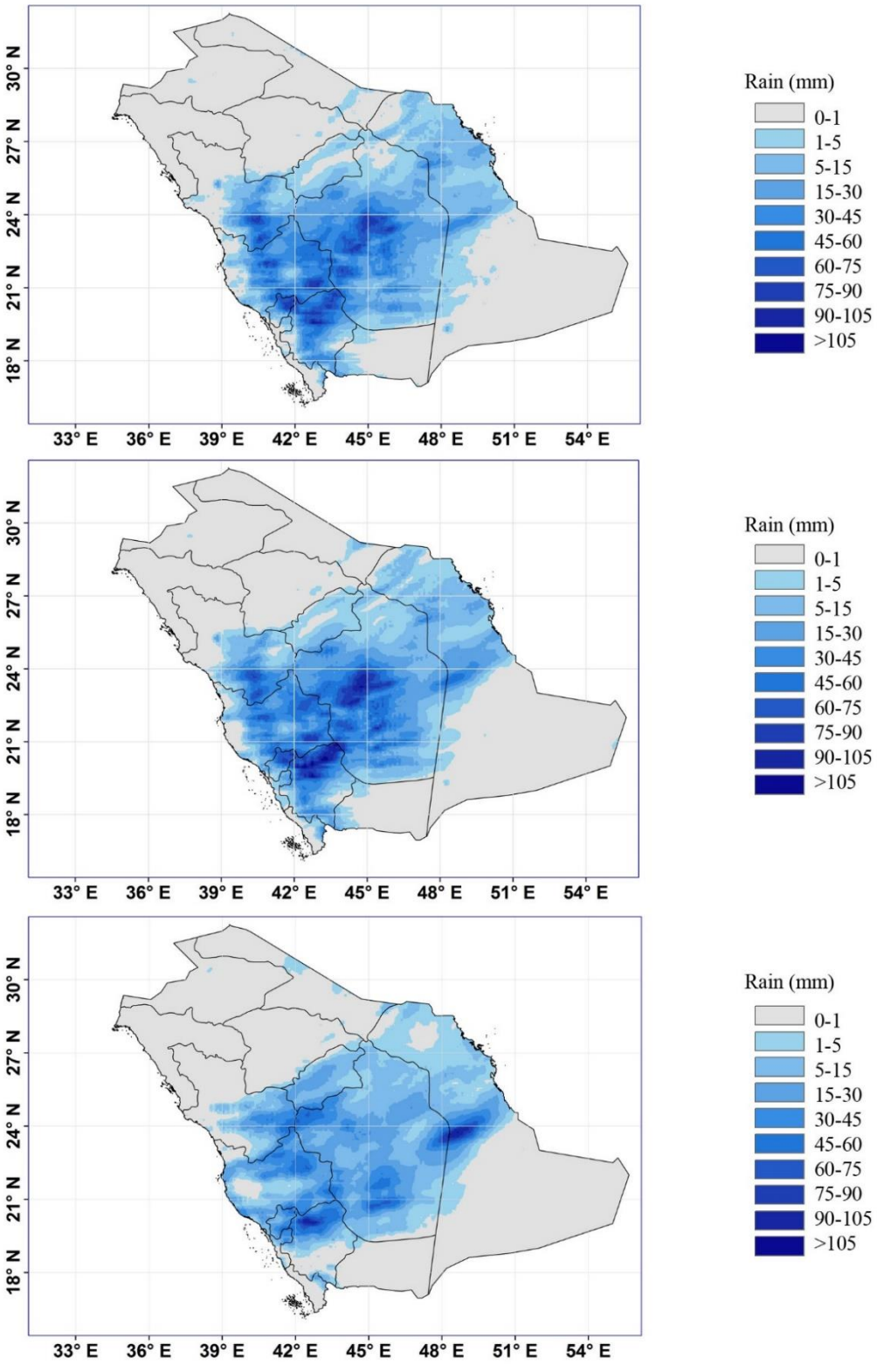

Figure B-10: The spatial distribution of the IMERG Early, Late and Final run precipitation products. (Date 12-04-2016)

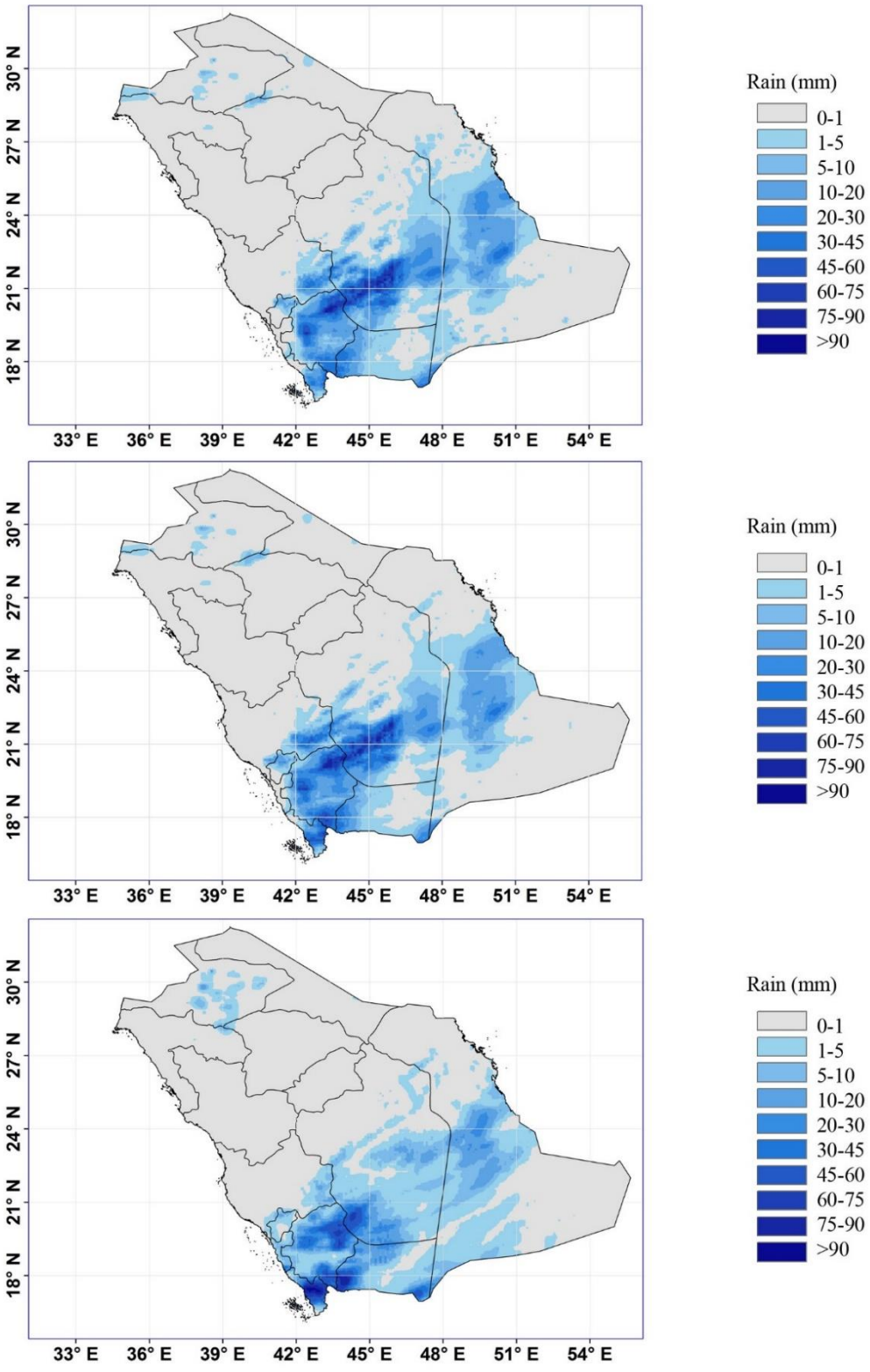

Figure B-11: The spatial distribution of the IMERG Early, Late and Final run precipitation products. (Date 13-04-2016)

Vitae

Name	: Mohammed Tarig Mohammed Mahmoud
Nationality	: Sudanese
Date of Birth	: 09/Oct./1990
Email	: eng.mohammedtarig@outlook.com
Address	: Khartoum - Sudan
Academic Background	: Civil Engineering